RSC Advances

PAPER

View Article Online
View Journal | View Issue

Cite this: *RSC Adv.*, 2017, **7**, 56496

Bioactivity-guided mixed synthesis and evaluation of α-alkenyl-γ and δ-lactone derivatives as potential fungicidal agents†

Yong-Ling Wu,[a] Yan-Qing Gao,[ab] De-Long Wang,[a] Chen-Quan Zhong,[a] Jun-Tao Feng *[ab] and Xing Zhang[ab]

Received 15th November 2017
Accepted 29th November 2017

DOI: 10.1039/c7ra12471f

rsc.li/rsc-advances

In view of the great antifungal activities of sesquiterpene lactones and natural product Tulipalin A, 52 derivatives derived from α-methylene-γ-butyrolactone substructures were synthesized to study antifungal activities. *In vitro* and *in vivo* antifungal activity results revealed that compounds **2-25**, which contain a γ-butyrolactone scaffold and cinnamic aldehyde moiety, have greater potent fungicidal activity than other compounds. The preliminary structure–activity relationships (SARs) demonstrated that compounds with electron-withdrawing groups and small steric hindrance would have more desirable potency. Meanwhile, the quantitative structure–activity relationship (QSAR) model ($R^2 = 0.947$, $F = 65.77$, and $S^2 = 0.0028$) revealed a convincing correlation of antifungal activity against *B. cinerea* with molecular structures of title compounds. The present study provided a more detailed insight into the antifungal activity of the α-methylene-γ-butyrolactone substructure, which provided a potential expectation for the exploration of α-alkenyl-γ-butyrolactone structures in agriculture.

Introduction

In recent years, fungicide resistance and food security problems have becoming increasingly serious.[1,2] Since it is difficult to find appropriate fungal-specific targets of fungal cells, the discovery of a new mode of action or novel fungicidal agents based on novel scaffolds from natural products has become important to overcome the chemical resistance problem. In fact, natural products with structural modification have been broadly used for discovering and developing pesticides in the market today, due to the structural diversities, environmental compatibilities, easy biodegradation, and lower environmental and mammalian toxicity characteristics.[3–6] In addition, discovering and screening candidates with antifungal activity from thousands of natural products is virtually and economically impossible, while employing a bioactivity-guided mixed synthesis method would reduce the problems with cost and time requirements for screening.

A wide variety of structures of sesquiterpene lactones (STLs) have a diversity of biological activities, such as cytotoxic, anticancer, antifungal, anti-inflammatory, and antimicrobial properties.[7–10] In fact, α-methylene-γ-lactone and cyclopentenone structures reacting with the sulfhydryl moieties of enzymes or functional proteins *via* the Michael type addition among numerous natural products are the important chemical scaffolds of STLs.[11,12] In our previous work, carabrone and its alcohol analogue carabrol, two known sesquiterpene lactones isolated from the fruits of *Carpesium macrocephalum*, were found to possess potent antifungal activity in a protective manner which blocked the early penetrative infection process of pathogenic spores.[13] The study of the structure–activity relationships (SARs) of carabrone derivates also revealed that the α-methylene-γ-butyrolactone core boosts their antifungal potency.[14,15] At the same time, Tulipalin A and B, two natural pharmacophores, both of which contain a methylene group, exerted great antimicrobial activities.[16] Therefore, as shown in Fig. 1, the bioactivity of these compounds guided us to continue to seek new analogous α-methylene-γ-lactone bearing templates with potent fungicidal efficacy.

α-Alkenyl-γ-butyrolactone derivates with a chain-ring have been demonstrated to reduce their cytotoxicity.[17] Moreover, little is known about the effect of the lactone ring conformation and constraints on the bio-activity of α-methylene-γ-lactone. Thus this prompted us to design and synthesize a series of α-alkenyl-γ-butyrolactone and δ-valerolactone derivates. Since the *in vitro* antifungal activity of fungicides does not always match the *in vivo* activity, *i.e.* in compounds with high *in vitro* antifungal activity, the *in vivo* activities were also tested. At the same time, SAR and constructed QSAR models were built to elaborate the relationship between structural features of the activity and mechanism actions.[18,19] The objective of this article was to seek an efficient candidate based on bioactivity-guided mixed synthesis.

[a]*Research and Development Center of Biorational Pesticide, Northwest A&F University, Yangling 712100, Shaanxi, China. E-mail: fengjt@nwsuaf.edu.cn; Fax: +86-29-87092122; Tel: +86-29-87092122*

[b]*Research Center of Biopesticide Technology & Engineering, Yangling 712100, Shaanxi, China*

† Electronic supplementary information (ESI) available. See DOI: 10.1039/c7ra12471f

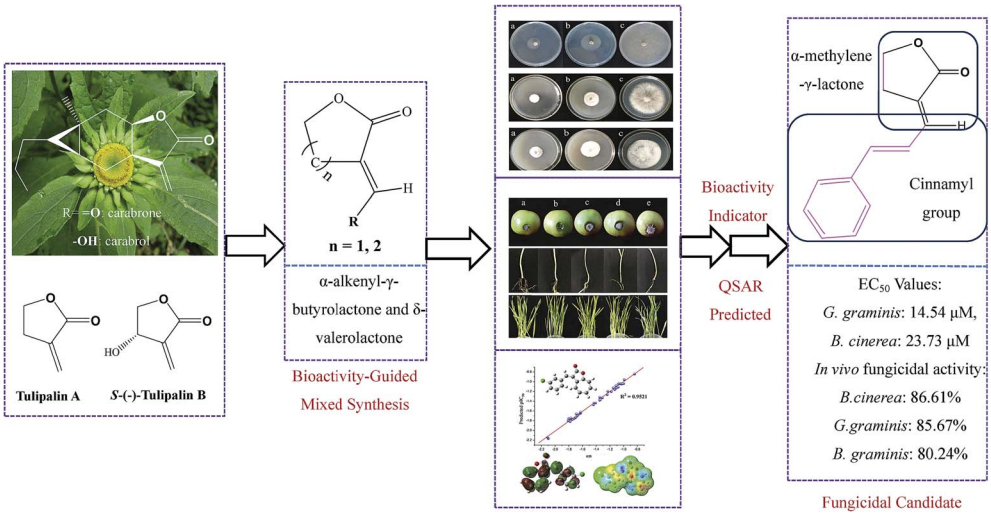

Fig. 1 The design strategy to find promising fungicidal candidates.

Experimental

Chemicals and instruments

Chemicals and reagents used in this research were of analytical grade (purchased from Aladdin Industrial Inc., Shanghai, China); all solvents were dried and redistilled before use. Analytical thin-layer chromatography (TLC) was performed on silica gel GF_{254}. Column chromatographic (CC) purification was carried out using silica gel (200–300 mesh), which was obtained from Qingdao Haiyang Chemical Co., Ltd. (Qingdao, China). The melting points of these synthetic derivatives were determined on an X-5 apparatus and uncorrected, and the apparatus was purchased from Beijing Tech. Nuclear magnetic resonance spectra (NMR) were obtained on a Bruker Avance 500 MHz instrument. HR-MS (ESI) was observed using a Bruker Apex-Ultra 7.0 T spectrometer. The reaction progress was monitored by thin-layer chromatography on silica gel GF-254 with detection by UV light.

Synthesis of compound α-alkenyl-γ-butyrolactone

As shown in Scheme 1, to a cooled (0 °C) solution of γ-butyrolactone (5.0 g, 58 mmol) and benzaldehyde (5.85 g, 55.1 mmol) in dry benzene (75 mL) was added KO*t*Bu (7.82 g, 69.7 mmol) portionwise.[20,21] After the addition, the thick orange solution was stirred at room temp for 6 h. The mixture was acidified with dilute H_2SO_4 (aq) and extracted with Et_2O (3 × 30 mL). The organic layer was dried ($MgSO_4$) and evaporated under reduced pressure. The residue was purified using flash column chromatography (silica gel, EtOAc/petroleum ether = 1 : 5) to yield **2** (5.4 g, 56%) as a white solid. The data of compound **2** is shown as follows.

Data for compound 2-1. White crystal; mp: 166.3–167.5 °C; 55% yield; ^{1}H NMR (500 MHz, $CDCl_3$) δ 7.39 (t, J = 3.0 Hz, 1H), 7.38–7.35 (m, 2H), 7.34–7.31 (m, 2H), 7.30–7.28 (m, 1H), 4.28 (s, 1H), 4.25 (s, 1H), 3.04 (td, J = 7.3, 2.9 Hz, 2H). ^{13}C NMR (126 MHz, $CDCl_3$): 172.37, 136.02, 134.62, 130.13, 129.72, 128.71, 124.02, 65.47, 27.27. HR-MS (ESI): m/z calcd for $C_{11}H_{10}O_2$ ([M + H]$^+$) 174.0861, found 175.0754.

Data for compound 2-2. White crystal; mp: 162.3–163.5 °C; 52% yield; ^{1}H NMR (500 MHz, $CDCl_3$) δ 7.68 (t, J = 2.9 Hz, 1H), 7.38 (dd, J = 7.6, 1.6 Hz, 1H), 7.27 (dt, J = 6.2, 3.1 Hz, 1H), 7.23–7.16 (m, 2H), 4.32–4.20 (m, 2H), 3.06–2.94 (m, 2H). ^{13}C NMR (126 MHz, $CDCl_3$): δ 172.10 135.20, 132.41, 131.68, 130.80, 129.98, 129.36, 127.23, 126.63, 68.01, 26.62. HR-MS (ESI): m/z calcd for $C_{11}H_9ClO_2$ ([M + Na]$^+$) 208.0291, found 231.0183.

Data for compound 2-3. White crystal; mp: 163.5–164.2 °C; 51% yield; ^{1}H NMR (500 MHz, $CDCl_3$) δ 7.68 (t, J = 2.9 Hz, 1H), 7.38 (dd, J = 7.6, 1.6 Hz, 1H), 7.27 (dt, J = 6.2, 3.1 Hz, 1H), 7.22–7.15 (m, 2H), 4.31–4.23 (m, 2H), 2.99 (ddd, J = 15.8, 10.0, 5.0 Hz, 2H). ^{13}C NMR (126 MHz, $CDCl_3$): 172.01, 135.20, 132.41, 131.68, 130.80, 129.98, 129.36, 127.26, 126.63, 69.22, 26.62. HR-MS (ESI): m/z calcd for $C_{11}H_9ClO_2$ ([M + Na]$^+$) 208.0291, found 231.0183.

Data for compound 2-4. White crystal; mp: 159.3–159.9 °C; 55% yield; ^{1}H NMR (500 MHz, $CDCl_3$) δ 7.53 (t, J = 2.9 Hz, 1H), 7.48–7.42 (m, 4H), 4.50 (t, J = 7.2 Hz, 2H), 3.25 (td, J = 7.3, 3.0 Hz, 2H). ^{13}C NMR (126 MHz, $CDCl_3$): 172.25, 135.85, 135.22, 133.14, 131.15, 129.25, 124.24, 65.44, 27.59. HR-MS (ESI): m/z calcd for $C_{11}H_9ClO_2$ ([M + Na]$^+$) 208.0291, found 231.0183.

Data for compound 2-5. White oil; 57% yield; ^{1}H NMR (500 MHz, $CDCl_3$) δ 7.57 (t, J = 2.9 Hz, 1H), 7.43 (dd, J = 8.1, 1.0 Hz, 1H), 7.33 (dd, J = 7.9, 1.2 Hz, 1H), 7.23 (dd, J = 11.3, 3.9 Hz, 1H), 7.06 (td, J = 7.9, 1.5 Hz, 1H), 4.20 (dt, J = 12.1, 5.8 Hz, 2H), 2.99–2.90 (m, 2H). ^{13}C NMR (126 MHz, $CDCl_3$): δ 171.89, 134.11, 133.25, 130.92, 129.52, 127.66, 127.58, 126.81, 125.68, 68.01, 29.41. HR-MS (ESI): m/z calcd for $C_{11}H_9BrO_2$ ([M + Na]$^+$) 251.9786, found 274.9678.

Data for compound 2-6. White crystal; mp: 161.5–162.2 °C; 44% yield; ^{1}H NMR (500 MHz, $CDCl_3$) δ 7.57 (t, J = 2.9 Hz, 1H), 7.43 (dd, J = 8.1, 1.0 Hz, 1H), 7.33 (dd, J = 7.9, 1.2 Hz, 1H), 7.23 (dd, J = 11.3, 3.9 Hz, 1H), 7.06 (td, J = 7.9, 1.5 Hz, 1H), 4.27 (dt, J = 12.1, 5.8 Hz, 2H), 2.96 (m, 2H). ^{13}C NMR (126 MHz, $CDCl_3$): δ 172.89, 133.11, 133.25, 130.92, 129.52, 128.66, 127.58, 125.81, 124.68, 66.01, 28.41. HR-MS (ESI): m/z calcd for $C_{11}H_9BrO_2$ ([M + Na]$^+$) 251.9786, found 274.9678.

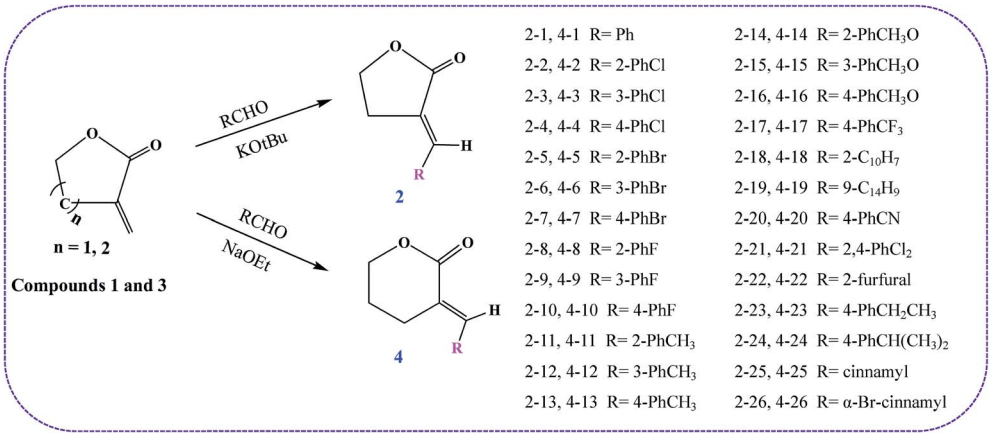

Scheme 1 Synthesis route of the target compounds **2-1–26** and **4-1–26**.

Data for compound 2-7. White crystal; mp: 166.2–167.2 °C; 57% yield; ^{1}H NMR (500 MHz, $CDCl_3$) δ 7.52 (t, J = 2.9 Hz, 1H), 7.35 (dd, J = 8.1, 1.0 Hz, 1H), 7.24 (dd, J = 7.9, 1.2 Hz, 1H), 7.21 (dd, J = 11.3, 3.9 Hz, 1H), 7.06 (td, J = 7.9, 1.5 Hz, 1H), 4.22 (dt, J = 12.1, 5.8 Hz, 2H), 3.03 (m, 2H). ^{13}C NMR (126 MHz, $CDCl_3$): δ 172.54, 135.13, 133.25, 131.63, 128.32, 127.63, 126.52, 125.82, 123.68, 65.03, 28.41. HR-MS (ESI): m/z calcd for $C_{11}H_9BrO_2$ ([M + Na]$^+$) 251.9786, found 274.9678.

Data for compound 2-8. White crystal; mp: 161.1–162.4 °C; 56% yield; ^{1}H NMR (500 MHz, $CDCl_3$) δ 7.47 (s, 1H), 7.24 (t, J = 9.6 Hz, 1H), 7.21 (dd, J = 11.3, 3.9 Hz, 1H), 7.06 (td, J = 7.9, 1.5 Hz, 1H), 6.97 (dd, J = 11.4, 5.5 Hz, 1H), 4.29 (t, J = 7.1 Hz, 2H), 3.04 (dd, J = 8.9, 4.6 Hz, 2H). ^{13}C NMR (126 MHz, $CDCl_3$): δ 172.35, 134.31, 133.31, 132.70, 131.93, 131.89, 123.54, 115.98, 112.81, 66.26, 28.38. HR-MS (ESI): m/z calcd for $C_{11}H_9FO_2$ ([M + Na]$^+$) 192.0587, found 215.0478.

Data for compound 2-9. White crystal; mp: 158.5–159.2 °C; 46% yield; ^{1}H NMR (500 MHz, $CDCl_3$) δ 7.45 (s, 1H), 7.30 (s, 1H), 7.27 (t, J = 9.6 Hz, 1H), 6.97 (dd, J = 11.4, 5.5 Hz, 2H), 4.27 (t, J = 7.1 Hz, 2H), 3.24 (dd, J = 8.9, 4.6 Hz, 2H). ^{13}C NMR (126 MHz, $CDCl_3$): δ 172.35, 135.64, 135.33, 134.72, 131.26, 131.61, 121.53, 115.98, 112.31, 66.29, 26.35. HR-MS (ESI): m/z calcd for $C_{11}H_9FO_2$ ([M + Na]$^+$) 192.0587, found 215.0478.

Data for compound 2-10. White crystal; mp: 161.3–162.6 °C; 53% yield; ^{1}H NMR (500 MHz, $CDCl_3$) δ 7.47–7.30 (m, 2H), 7.27 (t, J = 9.6 Hz, 1H), 6.97 (dd, J = 11.4, 5.5 Hz, 2H), 4.29 (t, J = 7.1 Hz, 2H), 3.04 (dd, J = 8.9, 4.6 Hz, 2H). ^{13}C NMR (126 MHz, $CDCl_3$): δ 172.35, 134.70, 131.96, 131.91, 123.54, 115.98, 115.81, 66.29, 27.35. HR-MS (ESI): m/z calcd for $C_{11}H_9FO_2$ ([M + Na]$^+$) 192.0587, found 215.0478.

Data for compound 2-11. White crystal; mp: 167.2–168.4 °C; 53% yield; ^{1}H NMR (500 MHz, $CDCl_3$) δ 7.38 (s, 1H), 7.13 (dd, J = 4.9, 3.9 Hz, 1H), 7.03–6.94 (m, 2H), 6.94–6.87 (m, 1H), 4.12–3.85 (m, 2H), 2.83–2.56 (m, 2H), 2.03 (d, J = 4.3 Hz, 3H). ^{13}C NMR (126 MHz, $CDCl_3$): δ 171.15, 138.19, 133.63, 132.61, 130.85, 129.36, 128.21, 126.45, 125.06, 67.38, 27.00, 21.90. HR-MS (ESI): m/z calcd for $C_{12}H_{12}O_2$ ([M + Na]$^+$) 188.0837, found 211.0730.

Data for compound 2-12. White crystal; mp: 155.5–156.4 °C; 56% yield; ^{1}H NMR (500 MHz, $CDCl_3$) δ 7.22 (d, J = 1.2 Hz, 1H), 7.15 (t, J = 7.6 Hz, 1H), 7.08 (d, J = 7.7 Hz, 1H), 7.05 (s, 1H), 7.02 (d, J = 7.5 Hz, 1H), 4.23–4.08 (m, 2H), 2.92 (dd, J = 9.6, 4.8 Hz, 2H), 2.18 (d, J = 15.2 Hz, 3H). ^{13}C NMR (126 MHz, $CDCl_3$): δ 172.31, 138.50, 135.79, 134.51, 130.75, 130.49, 128.55, 126.77, 123.71, 67.38, 29.13, 23.18. HR-MS (ESI): m/z calcd for $C_{12}H_{12}O_2$ ([M + Na]$^+$) 188.0837, found 211.0730.

Data for compound 2-13. White crystal; mp: 159.5–160.2 °C; 61% yield; ^{1}H NMR (500 MHz, $CDCl_3$) δ 7.55 (t, J = 2.9 Hz, 1H), 7.42 (d, J = 8.1 Hz, 2H), 7.27 (d, J = 8.0 Hz, 2H), 4.47 (t, J = 7.3 Hz, 2H), 3.24 (td, J = 7.3, 2.9 Hz, 2H), 2.42 (s, 3H). ^{13}C NMR (126 MHz, $CDCl_3$): δ 172.74, 140.37, 136.60, 131.93, 130.07, 129.72, 122.42, 65.45, 27.46, 21.51. HR-MS (ESI): m/z calcd for $C_{12}H_{12}O_2$ ([M + Na]$^+$) 188.0837, found 211.0730.

Data for compound 2-14. White crystal; mp: 161.5–162.2 °C; 57% yield; ^{1}H NMR (500 MHz, $CDCl_3$) δ 7.75 (t, J = 2.9 Hz, 1H), 7.24 (d, J = 7.7 Hz, 1H), 7.19 (t, J = 7.9 Hz, 1H), 6.82 (dd, J = 14.6, 7.1 Hz, 1H), 6.76 (t, J = 7.6 Hz, 1H), 4.18 (t, J = 7.3 Hz, 2H), 3.62 (d, J = 20.1 Hz, 3H), 2.92 (td, J = 7.3, 2.9 Hz, 2H). ^{13}C NMR (126 MHz, $CDCl_3$): δ 171.68, 160.74, 131.69, 130.57, 128.84, 123.36, 123.29, 120.45, 112.14, 69.22, 55.22, 27.29. HR-MS (ESI): m/z calcd for $C_{12}H_{12}O_3$ ([M + H]$^+$) 204.0786, found 205.0859.

Data for compound 2-15. White crystal; mp: 165.2–166.4 °C; 44% yield; ^{1}H NMR (500 MHz, $CDCl_3$) δ 7.21–7.06 (m, 2H), 6.82 (dd, J = 12.0, 7.7 Hz, 1H), 6.79–6.66 (m, 2H), 4.22–4.09 (m, 2H), 3.68–3.45 (m, 3H), 2.89 (dd, J = 9.1, 6.1 Hz, 2H). ^{13}C NMR (126 MHz, $CDCl_3$): δ 172.23, 159.61, 138.21, 135.53, 130.99, 124.29, 122.19, 115.18, 65.43, 54.98, 27.32. HR-MS (ESI): m/z calcd for $C_{12}H_{12}O_3$ ([M + H]$^+$) 204.0786, found 205.0859.

Data for compound 2-16. White crystal; mp: 161.5–162.2 °C; 54% yield; ^{1}H NMR (500 MHz, $CDCl_3$) δ 7.22 (d, J = 8.7 Hz, 2H), 7.18 (s, 1H), 6.73 (d, J = 8.8 Hz, 2H), 4.18 (t, J = 7.3 Hz, 2H), 3.57 (d, J = 31.6 Hz, 3H), 2.93 (td, J = 7.3, 2.5 Hz, 2H). ^{13}C NMR (126 MHz, $CDCl_3$): δ 172.60, 160.67, 135.03, 132.83, 126.85, 120.97, 115.62, 68.40, 55.05, 27.06. HR-MS (ESI): m/z calcd for $C_{12}H_{12}O_3$ ([M + H]$^+$) 204.0786, found 205.0859.

Data for compound 2-17. White crystal; mp: 162.5–163.1 °C; 45% yield; ^{1}H NMR (500 MHz, $CDCl_3$) δ 7.61 (d, J = 8.0 Hz, 2H), 7.58–7.52 (m, 2H), 7.45 (s, 1H), 4.41 (t, J = 7.1 Hz, 2H), 3.23 (dd, J = 26.6, 10.9 Hz, 2H). ^{13}C NMR (126 MHz, $CDCl_3$): δ 172.19,

137.98, 134.45, 130.14, 126.93, 125.94, 125.78, 67.66, 46.85, 27.43. HR-MS (ESI): *m/z* calcd for $C_{12}H_9F_3O_2$ ([M + Na]$^+$) 242.0555, found 265.0447.

Data for compound 2-18. White crystal; mp: 167.3–168.3 °C; 42% yield; ^{1}H NMR (500 MHz, $CDCl_3$) δ 7.96 (d, J = 6.2 Hz, 1H), 7.91–7.85 (m, 3H), 7.71 (t, J = 2.8 Hz, 1H), 7.59 (dd, J = 8.6, 1.5 Hz, 1H), 7.57–7.52 (m, 2H), 4.52–4.43 (m, 2H), 3.33 (td, J = 7.3, 2.9 Hz, 2H). ^{13}C NMR (126 MHz, $CDCl_3$): δ 173.28, 136.68, 133.62, 133.18, 132.18, 130.87, 128.62, 128.60, 127.72, 127.49, 126.81, 126.39, 123.76, 65.40, 27.60. HR-MS (ESI): *m/z* calcd for $C_{15}H_{12}O_2$ ([M + H]$^+$) 224.0837, found 225.0910.

Data for compound 2-19. White crystal; mp: 160.3–161.4 °C; 43% yield; ^{1}H NMR (500 MHz, $CDCl_3$) δ 8.46 (s, 1H), 8.43 (s, 1H), 8.06–8.00 (m, 2H), 7.97 (t, J = 7.4 Hz, 2H), 7.58–7.48 (m, 4H), 4.48–4.23 (m, 2H), 2.57 (td, J = 7.1, 3.2 Hz, 2H). ^{13}C NMR (126 MHz, $CDCl_3$): δ 171.06, 132.98, 131.27, 131.01, 129.16, 128.67, 128.62, 128.25, 126.57, 125.53, 125.17, 65.43, 26.95. HR-MS (ESI): *m/z* calcd for $C_{19}H_{14}O_2$ ([M + H]$^+$) 274.0994, found 275.1067.

Data for compound 2-20. White crystal; mp: 164.2–165.3 °C; 45% yield; ^{1}H NMR (500 MHz, $CDCl_3$) δ 10.14 (d, J = 1.4 Hz, 1H), 8.04 (dd, J = 8.2, 1.4 Hz, 2H), 7.88 (dd, J = 18.9, 12.1 Hz, 2H), 3.80–3.66 (m, 2H), 2.09 (d, J = 1.6 Hz, 2H). ^{13}C NMR (126 MHz, $CDCl_3$): δ 190.56, 139.24, 132.92, 132.25, 130.11, 129.90, 117.94, 52.29, 30.60. HR-MS (ESI): *m/z* calcd for $C_{12}H_9NO_2$ ([M + H]$^+$) 199.0633, found 200.0706.

Data for compound 2-21. White crystal; mp: 155.5–155.9 °C; 47% yield; ^{1}H NMR (500 MHz, $CDCl_3$) δ 7.53 (t, J = 2.9 Hz, 1H), 7.19 (t, J = 7.9 Hz, 1H), 6.86 (dd, J = 14.6, 7.1 Hz, 1H), 6.56 (t, J = 7.6 Hz, 1H), 4.12 (t, J = 7.3 Hz, 2H), 2.82 (td, J = 7.3, 2.9 Hz, 2H). ^{13}C NMR (126 MHz, $CDCl_3$): δ 172.64, 162.74, 134.69, 133.52, 124.83, 123.36, 121.25, 120.43, 113.14, 68.52, 56.24, 27.23. HR-MS (ESI): *m/z* calcd for $C_{11}H_8Cl_2O_2$ ([M + H]$^+$) 241.9901, found 242.9974.

Data for compound 2-22. White crystal; mp: 157.5–158.4 °C; 46% yield; ^{1}H NMR (500 MHz, $CDCl_3$) δ 7.48 (s, 1H), 7.16 (t, J = 2.6 Hz, 1H), 6.56 (d, J = 3.5 Hz, 1H), 6.43 (dd, J = 3.4, 1.7 Hz, 1H), 4.32 (t, J = 7.4 Hz, 2H), 3.12 (td, J = 7.3, 2.6 Hz, 2H). ^{13}C NMR (126 MHz, $CDCl_3$): δ 172.17, 151.19, 145.25, 122.48, 121.28, 115.73, 112.49, 65.63, 27.21. HR-MS (ESI): *m/z* calcd for $C_9H_8O_3$ ([M + H]$^+$) 164.0473, found 165.0546.

Data for compound 2-23. White crystal; mp: 166.5–167.2 °C; 43% yield; ^{1}H NMR (500 MHz, $CDCl_3$) δ 7.28 (t, J = 2.9 Hz, 1H), 7.21 (d, J = 8.3 Hz, 2H), 7.07 (dd, J = 13.9, 6.1 Hz, 2H), 4.17 (t, J = 7.3 Hz, 2H), 2.93 (td, J = 7.3, 2.9 Hz, 2H), 2.54–2.41 (m, 2H), 1.09 (t, J = 7.7 Hz, 3H). ^{13}C NMR (126 MHz, $CDCl_3$): δ 174.83, 146.25, 135.78, 131.95, 130.68, 128.41, 122.82, 68.58, 28.49, 27.22, 15.13. HR-MS (ESI): *m/z* calcd for $C_{13}H_{14}O_2$ ([M + H]$^+$) 202.0994, found 225.0886.

Data for compound 2-24. White crystal; mp: 154.2–155.3 °C; 43% yield; ^{1}H NMR (500 MHz, $CDCl_3$) δ 7.25 (d, J = 2.3 Hz, 1H), 7.23–7.13 (m, 2H), 7.12–6.96 (m, 2H), 4.13 (dd, J = 13.5, 6.4 Hz, 2H), 3.00–2.85 (m, 2H), 1.79 (t, J = 4.7 Hz, 1H), 1.08–1.01 (m, 6H). ^{13}C NMR (126 MHz, $CDCl_3$): δ 171.35, 150.69, 135.62, 132.10, 130.63, 128.51, 122.92, 65.23, 35.36, 26.95, 25.02. HR-MS (ESI): *m/z* calcd for $C_{14}H_{16}O_2$ ([M + H]$^+$) 216.1150, found 217.1223.

Data for compound 2-25. White crystal; mp: 161.2–162.4 °C; 55% yield; ^{1}H NMR (500 MHz, $CDCl_3$) δ 7.51 (dd, J = 8.9, 7.5 Hz, 2H), 7.42–7.37 (m, 2H), 7.35 (dt, J = 5.1, 2.0 Hz, 1H), 7.26 (dt, J = 11.2, 2.8 Hz, 1H), 6.94 (d, J = 15.6 Hz, 1H), 6.90–6.80 (m, 1H), 4.61–4.23 (m, 2H), 3.08 (td, J = 7.4, 2.6 Hz, 2H). ^{13}C NMR (126 MHz, $CDCl_3$): δ 171.97, 141.46, 135.99, 135.85, 129.35, 129.07, 127.35, 124.53, 123.84, 65.54, 25.70. HR-MS (ESI): *m/z* calcd for $C_{13}H_{12}O_2$ ([M + H]$^+$) 200.0837, found 201.0910.

Data for compound 2-26. White crystal; mp: 159.2–160.2 °C; 43% yield; ^{1}H NMR (500 MHz, $CDCl_3$) δ 7.71 (dd, J = 8.9, 7.5 Hz, 2H), 7.56–7.47 (m, 2H), 7.36 (dt, J = 5.1, 2.0 Hz, 1H), 7.16 (dt, J = 11.2, 2.8 Hz, 1H), 6.85 (d, J = 15.6 Hz, 1H), 4.65 (m, 2H), 3.08 (td, J = 7.4, 2.6 Hz, 2H). ^{13}C NMR (126 MHz, $CDCl_3$): δ 172.94, 143.45, 136.93, 135.84, 128.35, 128.07, 127.34, 124.73, 122.84, 65.64, 26.71. HR-MS (ESI): *m/z* calcd for $C_{13}H_{12}O_2$ ([M + H]$^+$) 277.9942, found 279.0015.

Synthesis of compound α-alkenyl-δ-valerolactone

A solution of aromatic aldehyde (5 mmol), δ-valerolactone (5 mmol) in anhydrous methyl alcohol was added dropwise to a methyl alcohol solution of NaOEt (10 mmol) under ice-cooling. The mixture was stirred at 0–10 °C for 3 hours. TLC was used to monitor whether the reaction was completed. Thereafter, the mixture was diluted with EtOAc, and acidified with dilute H_2SO_4 (aq). The organic layer was then washed with $NaHCO_3$ solution and water, dried with $MgSO_4$ and removed under reduced pressure to give the crude product which was purified by column chromatography with petroleum ether–EtOAc (10 : 1) to afford compound **4**. The structures of all compounds were confirmed by ^{1}H and ^{13}C NMR and HR-MS analyses. The synthesis route is shown in Scheme 1 and the data of compound **4** is shown as follows.

Data for compound 4-1. White crystal; mp: 167.4–168.3 °C; 45% yield; ^{1}H NMR (500 MHz, $CDCl_3$) δ 7.66 (s, 1H), 7.46 (s, 1H), 7.28 (s, 1H), 7.17 (m, 3H), 4.22 (m, 2H), 2.71 (m, 2H), 1.76 (m, 2H). ^{13}C NMR (126 MHz, $CDCl_3$): δ 168.23, 138.34, 136.66, 136.21, 129.21, 128.98, 128.67, 128.54, 128.59, 74.05, 27.20, 24.10. HR-MS (ESI): *m/z* calcd for $C_{12}H_{12}O_2$ ([M + H]$^+$) 188.0837, found 189.0910.

Data for compound 4-2. White crystal; mp: 162.3–163.2 °C; 44% yield; ^{1}H NMR (500 MHz, $CDCl_3$) δ 7.59 (s, 1H), 7.16 (s, 1H), 7.11–7.09 (m, 3H), 4.29–4.09 (m, 2H), 2.72–2.55 (m, 2H), 1.76–1.72 (m, 2H). ^{13}C NMR (126 MHz, $CDCl_3$): δ 169.63, 138.38, 135.56, 135.41, 129.71, 129.18, 128.82, 128.13, 127.55, 72.65, 27.23, 23.12. HR-MS (ESI): *m/z* calcd for $C_{12}H_{11}ClO_2$ ([M + H]$^+$) 222.0448, found 223.0521.

Data for compound 4-3. White crystal; mp: 156.5–157.7 °C; 47% yield; ^{1}H NMR (500 MHz, $CDCl_3$) δ 7.56 (s, 1H), 7.18 (s, 1H), 7.14–7.09 (m, 3H), 4.29–4.09 (m, 2H), 2.73–2.56 (m, 2H), 1.78–1.70 (m, 2H). ^{13}C NMR (126 MHz, $CDCl_3$): δ 167.23, 139.35, 136.52, 134.51, 129.81, 129.58, 128.82, 128.24, 127.59, 72.05, 28.20, 24.10. HR-MS (ESI): *m/z* calcd for $C_{12}H_{11}ClO_2$ ([M + H]$^+$) 222.0448, found 223.0521.

Data for compound 4-4. White crystal; mp: 158.8–159.2 °C; 43% yield; ^{1}H NMR (500 MHz, $CDCl_3$) δ 7.55 (d, J = 2.1 Hz, 1H), 7.16–7.12 (m, 5H), 4.23–4.06 (m, 2H), 2.59 (dd, J = 8.7, 4.4 Hz,

2H), 1.77–1.68 (m, 2H). ^{13}C NMR (126 MHz, $CDCl_3$): δ 168.60, 141.05, 133.37, 131.68, 130.69, 128.91, 126.60, 68.76, 26.81, 24.10. HR-MS (ESI): *m*/*z* calcd for $C_{12}H_{11}ClO_2$ ($[M + H]^+$) 222.0448, found 223.0521.

Data for compound 4-5. White crystal; mp: 162.3–163.4 °C; 46% yield; ^{1}H NMR (500 MHz, $CDCl_3$) δ 7.56–7.46 (m, 1H), 7.42–7.35 (m, 1H), 7.27–7.16 (m, 2H), 7.03 (td, J = 7.2, 3.7 Hz, 1H), 4.31–4.11 (m, 2H), 2.60–2.44 (m, 2H), 1.82–1.70 (m, 2H). ^{13}C NMR (126 MHz, $CDCl_3$): δ 172.32, 133.17, 132.47, 130.54, 128.77, 127.53, 124.52, 120.97, 70.82, 45.35, 26.58, 22.84. HR-MS (ESI): *m*/*z* calcd for $C_{12}H_{11}BrO_2$ ($[M + Na]^+$) 265.9942, found 288.9834.

Data for compound 4-6. White crystal; mp: 160.5–161.2 °C; 42% yield; ^{1}H NMR (500 MHz, $CDCl_3$) δ 7.50–7.46 (m, 1H), 7.40 (d, J = 8.1 Hz, 1H), 7.34–7.30 (m, 1H), 7.29 (t, J = 3.0 Hz, 1H), 7.22 (t, J = 7.8 Hz, 1H), 4.42–4.26 (m, 2H), 3.10 (tt, J = 28.8, 14.4 Hz, 2H), 2.19–2.10 (m, 2H). ^{13}C NMR (126 MHz, $CDCl_3$): δ 172.12, 136.62, 134.46, 132.63, 132.38, 130.97, 128.57, 125.46, 123.28, 69.39, 67.38, 28.20. HR-MS (ESI): *m*/*z* calcd for $C_{12}H_{11}BrO_2$ ($[M + Na]^+$) 265.9942, found 288.9834.

Data for compound 4-7. White crystal; mp: 166.1–166.8 °C; 42% yield; ^{1}H NMR (500 MHz, $CDCl_3$) δ 7.62–7.56 (m, 2H), 7.51 (dd, J = 6.1, 3.2 Hz, 1H), 7.38 (d, J = 8.5 Hz, 2H), 4.50 (t, J = 7.2 Hz, 2H), 3.24 (td, J = 7.3, 2.9 Hz, 2H), 2.43–1.91 (m, 0H). ^{13}C NMR (126 MHz, $CDCl_3$): δ 172.24, 135.30, 133.56, 132.22, 131.33, 124.43, 124.23, 65.45, 27.61. HR-MS (ESI): *m*/*z* calcd for $C_{12}H_{11}BrO_2$ ($[M + Na]^+$) 265.9942, found 288.9834.

Data for compound 4-8. White crystal; mp: 167.2–168.5 °C; 43% yield; ^{1}H NMR (500 MHz, $CDCl_3$) δ 7.67 (d, J = 1.9 Hz, 1H), 7.43 (m, 1H), 7.28 (s, 1H), 7.13 (m, 2H), 4.57–4.34 (m, 2H), 2.98–2.72 (m, 2H), 1.96 (m, 2H). ^{13}C NMR (126 MHz, $CDCl_3$): δ 168.41, 142.34, 140.36, 132.24, 131.12, 125.56, 123.43, 115.83, 115.53, 67.26, 27.61, 21.89. HR-MS (ESI): *m*/*z* calcd for $C_{12}H_{11}FO_2$ ($[M + Na]^+$) 206.0743, found 229.0635.

Data for compound 4-9. White crystal; mp: 152.5–153.3 °C; 42% yield; ^{1}H NMR (500 MHz, $CDCl_3$) δ 7.85 (d, J = 1.9 Hz, 1H), 7.43–7.32 (m, 2H), 7.28 (s, 1H), 7.13 (m, 2H), 4.45 (m, 2H), 2.96 (m, 2H), 1.96 (m, 2H). ^{13}C NMR (126 MHz, $CDCl_3$): δ 166.73, 142.34, 140.21, 132.24, 132.18, 125.56, 125.21, 115.63, 112.73, 68.61, 27.53, 22.43. HR-MS (ESI): *m*/*z* calcd for $C_{12}H_{11}FO_2$ ($[M + Na]^+$) 206.0743, found 229.0635.

Data for compound 4-10. White crystal; mp: 158.3–159.2 °C; 44% yield; ^{1}H NMR (500 MHz, $CDCl_3$) δ 7.77 (d, J = 1.9 Hz, 1H), 7.45–7.32 (m, 2H), 7.10–6.97 (m, 2H), 4.47–4.24 (m, 2H), 2.94–2.70 (m, 2H), 1.93–1.82 (m, 2H). ^{13}C NMR (126 MHz, $CDCl_3$): δ 167.71, 141.33, 132.24, 132.18, 125.56, 116.03, 115.53, 68.66, 27.57, 22.83. HR-MS (ESI): *m*/*z* calcd for $C_{12}H_{11}FO_2$ ($[M + Na]^+$) 206.0743, found 229.0635.

Data for compound 4-11. White crystal; mp: 157.5–157.9 °C; 46% yield; ^{1}H NMR (500 MHz, $CDCl_3$) δ 8.02 (s, 1H), 7.28–7.20 (m, 4H), 4.56–4.31 (m, 2H), 2.72 (td, J = 6.7, 2.2 Hz, 2H), 2.34–2.20 (m, 3H), 1.93 (td, J = 11.4, 6.1 Hz, 2H). ^{13}C NMR (126 MHz, $CDCl_3$): δ 166.65, 140.58, 137.61, 134.00, 130.36, 128.87, 128.58, 126.65, 125.55, 69.96, 26.04, 23.43, 20.43. HR-MS (ESI): *m*/*z* calcd for $C_{13}H_{14}O_2$ ($[M + H]^+$) 202.0994, found 203.0167.

Data for compound 4-12. White crystal; mp: 161.5–162.2 °C; 42% yield; ^{1}H NMR (500 MHz, $CDCl_3$) δ 7.79 (t, J = 2.2 Hz, 1H), 7.23 (t, J = 7.5 Hz, 1H), 7.16 (t, J = 7.8 Hz, 2H), 7.10 (d, J = 7.4 Hz, 1H), 4.42–4.20 (m, 2H), 2.79 (td, J = 6.6, 2.3 Hz, 2H), 2.29 (d, J = 8.8 Hz, 3H), 1.87 (td, J = 11.2, 6.4 Hz, 2H). ^{13}C NMR (126 MHz, $CDCl_3$): δ 166.91, 141.44, 138.51, 134.85, 130.81, 130.41, 128.74, 127.80, 124.96, 70.78, 25.89, 23.46, 22.25. HR-MS (ESI): *m*/*z* calcd for $C_{13}H_{14}O_2$ ($[M + H]^+$) 202.0994, found 203.0167.

Data for compound 4-13. White crystal; mp: 157.5–158.2 °C; 47% yield; ^{1}H NMR (500 MHz, $CDCl_3$) δ 7.78 (s, 1H), 7.31 (dd, J = 50.5, 26.7 Hz, 2H), 6.88 (d, J = 8.5 Hz, 2H), 4.45–4.23 (m, 2H), 3.90–3.71 (m, 3H), 2.79 (s, 2H), 1.92 (dd, J = 17.7, 12.1 Hz, 2H). ^{13}C NMR (126 MHz, $CDCl_3$): δ 167.31, 159.71, 141.16, 134.10, 130.35, 123.26, 116.89, 68.48, 57.67, 26.28, 24.73. HR-MS (ESI): *m*/*z* calcd for $C_{13}H_{14}O_2$ ($[M + H]^+$) 202.0994, found 203.0167.

Data for compound 4-14. White crystal; mp: 165.3–166.2 °C; 46% yield; ^{1}H NMR (500 MHz, $CDCl_3$) δ 7.76 (d, J = 1.9 Hz, 1H), 7.31 (m, 1H), 6.98 (d, J = 7.3 Hz, 1H), 6.88 (s, 1H), 6.81 (dd, J = 4.4, 3.8 Hz, 1H), 4.26 (dd, J = 10.2, 5.1 Hz, 2H), 3.72 (t, J = 12.5 Hz, 3H), 2.71 (d, J = 3.8 Hz, 2H), 1.91 (m, 2H). ^{13}C NMR (126 MHz, $CDCl_3$): δ 165.67, 158.15, 142.52, 135.45, 128.44, 126.54, 123.53, 114.67, 112.53, 68.63, 55.21, 26.86, 23.90. HR-MS (ESI): *m*/*z* calcd for $C_{13}H_{14}O_3$ ($[M + H]^+$) 218.0943, found 219.1016.

Data for compound 4-15. White crystal; mp: 161.2–162.4 °C; 43% yield; ^{1}H NMR (500 MHz, $CDCl_3$) δ 7.77 (d, J = 1.9 Hz, 1H), 7.32–7.10 (m, 1H), 6.94 (d, J = 7.3 Hz, 1H), 6.87 (s, 1H), 6.83 (dd, J = 4.4, 3.8 Hz, 1H), 4.29 (dd, J = 10.2, 5.1 Hz, 2H), 3.75 (t, J = 12.5 Hz, 3H), 2.78 (d, J = 3.8 Hz, 2H), 1.93 (m, 2H). ^{13}C NMR (126 MHz, $CDCl_3$): δ 166.76, 159.18, 141.12, 136.15, 129.40, 126.24, 122.54, 115.67, 114.64, 68.67, 55.22, 25.86, 22.90. HR-MS (ESI): *m*/*z* calcd for $C_{13}H_{14}O_3$ ($[M + H]^+$) 218.0943, found 219.1016.

Data for compound 4-16. White crystal; mp: 152.5–153.2 °C; 42% yield; ^{1}H NMR (500 MHz, $CDCl_3$) δ 7.78 (s, 1H), 7.34 (t, J = 16.1 Hz, 2H), 6.88 (d, J = 8.5 Hz, 2H), 4.42–4.12 (m, 2H), 3.95–3.60 (m, 3H), 2.79 (s, 2H), 1.92 (dd, J = 17.7, 12.1 Hz, 2H). ^{13}C NMR (126 MHz, $CDCl_3$): δ 167.31, 160.37, 141.16, 133.82, 129.07, 123.26, 115.97, 68.48, 56.40, 25.19, 23.26. HR-MS (ESI): *m*/*z* calcd for $C_{13}H_{14}O_3$ ($[M + H]^+$) 218.0943, found 219.1016.

Data for compound 4-17. White crystal; mp: 158.1–159.5 °C; 45% yield; ^{1}H NMR (500 MHz, $CDCl_3$) δ 7.70 (d, J = 7.0 Hz, 1H), 7.53–7.45 (m, 2H), 7.38 (d, J = 7.5 Hz, 2H), 4.21 (dd, J = 26.4, 16.2 Hz, 2H), 2.81–2.59 (m, 2H), 1.85–1.74 (m, 2H). ^{13}C NMR (126 MHz, $CDCl_3$): δ 166.36, 139.19, 138.29, 130.53, 128.37, 125.07, 125.07, 68.73, 27.21, 23.18. HR-MS (ESI): *m*/*z* calcd for $C_{13}H_{11}F_3O_2$ ($[M + H]^+$) 256.0711, found 257.0784.

Data for compound 4-18. White crystal; mp: 157.7–158.5 °C; 42% yield; ^{1}H NMR (500 MHz, $CDCl_3$) δ 8.05 (s, 1H), 7.85–7.79 (m, 4H), 7.53–7.47 (m, 4H), 4.45–4.34 (m, 2H), 2.89 (dd, J = 8.4, 4.4 Hz, 2H), 1.93–1.85 (m, 2H). ^{13}C NMR (126 MHz, $CDCl_3$): δ 167.14, 141.35, 133.24, 133.02, 132.45, 130.45, 128.55, 128.18, 127.66, 127.25, 127.19, 126.62, 126.02, 68.76, 26.01, 24.38. HR-MS (ESI): *m*/*z* calcd for $C_{16}H_{14}O_2$ ($[M + H]^+$) 238.0994, found 239.1067.

Data for compound 4-19. White crystal; mp: 161.2–161.7 °C; 43% yield; ^{1}H NMR (500 MHz, $CDCl_3$) δ 8.41 (s, 1H), 8.40 (s, 1H), 8.06–8.00 (m, 2H), 7.93 (t, J = 7.4 Hz, 2H), 7.52–7.48 (m, 4H), 4.48–4.23 (m, 2H), 2.55 (td, J = 7.1, 3.2 Hz, 2H), 1.85–1.74 (m, 2H). ^{13}C NMR (126 MHz, $CDCl_3$): δ 172.36, 133.92, 131.57, 131.01, 129.86, 128.43, 128.54, 128.25, 126.57, 125.21, 125.11,

66.44, 26.65. HR-MS (ESI): *m*/*z* calcd for $C_{20}H_{16}O_2$ ($[M + H]^+$) 288.1150, found 289.1223.

Data for compound 4-20. White crystal; mp: 159.6–160.4 °C; 43% yield; ^{1}H NMR (500 MHz, $CDCl_3$) δ 10.03 (d, J = 1.4 Hz, 1H), 8.21 (dd, J = 8.2, 1.4 Hz, 2H), 7.86 (dd, J = 18.9, 12.1 Hz, 2H), 3.82–3.66 (m, 2H), 2.53 (d, J = 1.6 Hz, 2H), 1.82 (m, 2H). ^{13}C NMR (126 MHz, $CDCl_3$): δ 193.33, 138.21, 132.73, 132.22, 130.41, 129.90, 118.54, 54.24, 32.63. HR-MS (ESI): *m*/*z* calcd for $C_{13}H_{11}NO_2$ ($[M + H]^+$) 213.0790, found 214.0863.

Data for compound 4-21. White crystal; mp: 158.5–159.5 °C; 42% yield; ^{1}H NMR (500 MHz, $CDCl_3$) δ 7.47 (t, J = 10.5 Hz, 1H), 7.30 (t, J = 2.9 Hz, 1H), 7.20–7.12 (m, 4H), 6.81 (dd, J = 19.0, 7.8 Hz, 1H), 4.23 (ddd, J = 15.9, 10.1, 5.4 Hz, 3H), 3.70 (dd, J = 7.2, 1.4 Hz, 2H), 1.96–1.84 (m, 2H). ^{13}C NMR (126 MHz, $CDCl_3$): δ 157.71, 136.60, 130.96, 130.69, 129.81, 129.53, 126.94, 121.28, 111.86, 56.68, 44.27, 25.90. HR-MS (ESI): *m*/*z* calcd for $C_{12}H_{10}Cl_2O_2$ ($[M + H]^+$) 256.0058, found 257.0131.

Data for compound 4-22. White crystal; mp: 161.5–162.4 °C; 43% yield; ^{1}H NMR (500 MHz, $CDCl_3$) δ 7.43 (s, 1H), 7.21 (t, J = 2.6 Hz, 1H), 6.52 (d, J = 3.5 Hz, 1H), 6.41 (dd, J = 3.4, 1.7 Hz, 1H), 4.32 (t, J = 7.4 Hz, 2H), 3.32 (td, J = 7.3, 2.6 Hz, 2H), 2.06–1.96 (m, 2H). ^{13}C NMR (126 MHz, $CDCl_3$): δ 171.87, 152.23, 142.21, 123.55, 121.18, 116.32, 112.49, 66.83, 46.63, 21.23. HR-MS (ESI): *m*/*z* calcd for $C_{10}H_{10}O_3$ ($[M + H]^+$) 178.0630, found 179.0703.

Data for compound 4-23. White crystal; mp: 161.6–162.3 °C; 41% yield; ^{1}H NMR (500 MHz, $CDCl_3$) δ 7.69 (d, J = 81.8 Hz, 1H), 7.40–7.21 (m, 2H), 7.14 (d, J = 8.1 Hz, 2H), 4.30–4.20 (m, 2H), 2.76 (dd, J = 6.1, 3.9 Hz, 2H), 2.64–2.53 (m, 2H), 1.88–1.79 (m, 2H), 1.15 (td, J = 7.5, 3.8 Hz, 3H). ^{13}C NMR (126 MHz, $CDCl_3$): δ 166.94, 145.64, 141.25, 132.61, 132.26, 127.89, 126.59, 68.52, 23.46, 16.23. HR-MS (ESI): *m*/*z* calcd for $C_{14}H_{16}O_2$ ($[M + H]^+$) 216.1150, found 217.1223.

Data for compound 4-24. White crystal; mp: 152.2–153.5 °C; 41% yield; ^{1}H NMR (500 MHz, $CDCl_3$) δ 7.27 (d, J = 2.3 Hz, 1H), 7.21–7.10 (m, 2H), 7.10 (m, 2H), 4.11 (dd, J = 13.5, 6.4 Hz, 2H), 3.03–2.82 (m, 2H), 2.11–1.96 (m, 2H). 1.77 (t, J = 4.7 Hz, 1H), 1.03–1.02 (m, 6H). ^{13}C NMR (126 MHz, $CDCl_3$): δ 172.35, 153.54, 137.65, 132.10, 131.32, 128.51, 121.92, 66.23, 35.36, 27.76, 24.03. HR-MS (ESI): *m*/*z* calcd for $C_{15}H_{18}O_2$ ($[M + H]^+$) 230.1307, found 231.1380.

Data for compound 4-25. White crystal; mp: 157.7–158.4 °C; 44% yield; ^{1}H NMR (500 MHz, $CDCl_3$) δ 7.56 (dd, J = 8.9, 7.5 Hz, 2H), 7.44–7.32 (m, 2H), 7.32 (dt, J = 5.1, 2.0 Hz, 1H), 7.28 (dt, J = 11.2, 2.8 Hz, 1H), 6.94 (d, J = 15.6 Hz, 1H), 6.91–6.80 (m, 1H), 4.63–4.23 (m, 2H), 3.18 (td, J = 7.4, 2.6 Hz, 2H), 1.96–1.95 (m, 2H). ^{13}C NMR (126 MHz, $CDCl_3$): δ 172.67, 142.54, 136.91, 132.55, 128.35, 129.07, 126.35, 122.53, 121.84, 66.54, 24.72. HR-MS (ESI): *m*/*z* calcd for $C_{14}H_{14}O_2$ ($[M + H]^+$) 214.0994, found 215.1067.

Data for compound 4-26. White crystal; mp: 157.3–158.8 °C; 43% yield; ^{1}H NMR (500 MHz, $CDCl_3$) δ 7.72 (dd, J = 8.9, 7.5 Hz, 2H), 7.54–7.41 (m, 2H), 7.32 (dt, J = 5.1, 2.0 Hz, 1H), 7.26 (dt, J = 11.2, 2.8 Hz, 1H), 6.86 (d, J = 15.6 Hz, 1H), 4.63 (m, 2H), 3.18 (td, J = 7.4, 2.6 Hz, 2H), 2.13–1.65 (m, 2H). ^{13}C NMR (126 MHz, $CDCl_3$): δ 173.94, 147.43, 135.93, 135.24, 129.15, 126.17, 125.14, 122.73, 121.84, 65.64, 25.71. HR-MS (ESI): *m*/*z* calcd for $C_{14}H_{12}BrO_2$ ($[M + H]^+$) 292.0099, found 293.0172.

Biological assays

Fungi. The pathogenic fungi *Botrytis cinerea*, *Colletotrichum lagenarium*, *Fusarium graminearum*, *Gaeumannomyces graminis var. tritici*, and *Sclerotinia sclerotiorum* were provided by the Center of Pesticide Research, Northwest A&F University, China. These fungi were grown on potato dextrose agar (PDA) plates at 25 °C and maintained at 4 °C with periodic subculturing.

In vitro antifungal assay

According to the mycelium linear growth rate method reported previously,[22–24] the *in vitro* antifungal activities of compounds against five strains of plant pathogenic fungi were tested.

The compounds with higher initial activities against *B. cinerea* and *G. graminis var. tritici* were selected to assay 50% inhibition concentration values (IC_{50}). In order to get a series of stock solutions, the test compound (2 mM) was diluted with 5% DMSO aqueous solution by a double-fold dilution method. Each stock solution (10 mL) was mixed with the autoclaved PDA medium (190 mL) to provide a set of mediums with different concentrations of the test compound (3.125, 6.25, 12.5, 25, 50 and 100 μM). The culture medium containing only 0.25% DMSO was used as a blank control, and Tulipalin A, carabrone and carbendazim were used as positive controls. Each test was performed in triplicate. Antifungal toxicity regression equations and IC_{50} values were established according to the method previously reported.[14]

In vivo antifungal assay

Fungi strains and fungicides. The fungal pathogens *B. cinerea*, *G. graminis* and *B. graminis* were provided by the Agricultural Culture Collection of China (Yangling, Shaanxi, China). *B. cinerea* and *G. graminis* were cultured for 2 weeks at 25 °C on potato dextrose agar (PDA) after being retrieved from the storage tube.

The stock solution of the test compound was diluted with water containing 0.1% tween-80 to 200 μg mL^{-1}.

Against *B. cinerea*. The protective activity of test samples against *B. cinerea* on tomato fruits was determined with the following methods. Tomato fruits were surface disinfected in sodium hypochlorite (7%, w/v) solution for 5 min and washed thoroughly with sterile water, then samples were spray tested on the tomato fruits until liquid flowed on the surface at 24 h before inoculation. Inoculated fruits were placed in plastic boxes at 25 °C with a 16 h photoperiod and 80% relative humidity for disease development, and carbendazim was used as the positive control. After 3 days, the average lesion diameter was determined by measuring each lesion in two perpendicular directions. The lengths of the long and short axes were averaged and disease control efficacy was calculated as follows: disease control efficacy = (lesion diameter in the water control − lesion diameter in the treatment)/lesion diameter in the water control × 100.

Against *G. graminis*.[25] *G. graminis* agar plugs (4 mm diameter) were taken from the growing edges of 7 day old PDA cultures of each isolate. The wheat seeds were surface disinfected in sodium hypochlorite (0.5%, v/v) for 4 min, and after

that the seeds were placed in tested samples for 30 min and put on top of the agar plug with each isolate culture, then covered with 2 cm thick sand in 9 cm diameter sterile plates. Triadimefon was used as the control. There were three replicates of each isolate and each replicate consisted of nine wheat seedlings. The seedlings were kept moist and at room temperature at 21 °C. The percentage of the affected root area was calculated after 21–25 days inoculation. Disease severity was recorded on a 0–4 visual scale of the rhizomes and roots, in which 0 = rhizomes and roots with no symptoms, 1 = lesions on <25%, 2 = lesions on 25–50%, 3 = lesions on 50–75%, and 4 = lesions on 75–100%. The disease index and biocontrol effect meet the following equation.

Against *B. graminis*.[26] Wheat seeds were surface disinfected in sodium hypochlorite (7%, w/v) solution for 5 min, washed thoroughly with sterile water, then germinated in 9 cm pots. After 14 days, the plants reached the desired leaf stage, and the tested samples were uniformly sprayed on the leaves 24 h before shaking the spores. After inoculation, the plants were incubated at 20 °C/15 °C in a growth chamber with cycles of 16 h light and 8 h darkness. Two controls were included in each experiment: untreated leaves and leaves treated with 15% triadimefon. Assessment of disease was made 7 days after inoculation by counting the number of colonies on 2.5 cm of the middle part of the treated leaf area. In most cases, leaves with colonies were assessed visually and classified according to a scale from 0 to 4, in which 0 = leaves with no symptoms, 1 = lesions on <25%, 2 = lesions on 25–50%, 3 = lesions on 50–75%, and 4 = lesions on 75–100%. The disease index and biocontrol effect meet the following equation.

$$\text{Disease index}(\%) = \frac{\sum(\text{grade of disease severity} \times \text{diseased plants of this grade})}{\text{total plants that were assessed} \times \text{the highest grade of disease severity}} \times 100$$

$$\text{Biocontrol effect}(\%) = \frac{\text{disease index of pathogen control} - \text{disease index of bacteria treatment}}{\text{disease index of pathogen control}} \times 100$$

Building and validation of the QSAR model

Building and validation of the QSAR model was carried out with a common procedure. Briefly, using the Gaussian 03W package of programs (Gaussian Inc.), the optimal conformers of the title compounds with the lowest energy were computed at the DFT/6-31G (d) level.[27] Meanwhile, the most stable configurations of the compounds were generated and the corresponding ".log" and ".chk" files were gained. Afterwards, the calculated results were transformed into a form compatible with CODESSA 2.7.15 using Ampac 9.1.3.[28,29] At last, all of the molecular descriptors involved in these compounds were calculated by CODESSA 2.7.15, and the heuristic analysis method was used to build the QSAR model, which determines the most significant structural features for antifungal activity against *B. cinerea*. During the model development process, the squared correction coefficient (R^2), the squared standard error of the estimates (S^2), and the Fisher significance ratio (F) were used to clarify the standards of statics. Moreover, the tested IC_{50} values were converted into the corresponding plog IC_{50} values and used as dependent variables to get better linear regression. The quality of the final model was ensured using internal validation and the "leave-one-out" cross-validation methods.[30,31]

Results and discussion

Chemistry

The synthetic routes of the title compounds are outlined in Scheme 1. To evaluate the essentiality of the substituent on the exocyclic carbon–carbon double bond of γ-lactone and δ-lactone, we synthesized a series of α-methylene-γ-lactone and α-methylene-δ-lactone compounds. γ-Butyrolactone and δ-valerolactone compounds were reacted with different substituent aldehydes, carried out in an ice-cooling bath under KO*t*Bu or NaOEt catalysts. With these concise and stereospecific methods, the stereochemistry of the exocyclic double bond was exclusively *E* in moderate yields. It is worth noting that the yield of the γ-butyrolactone derivates (44–61%) was obviously higher than that of the δ-valerolactone derivates (41–47%), which may be due to the ring tension of the former lactone compounds being lower than that of the latter, and results in the γ-butyrolactone derivates tending to be more stable.

Antifungal activity and SARs

The *in vitro* screening results of the title compounds for preliminary antifungal activities against five pathogenic fungi (*Botrytis cinerea*, *Colletotrichum lagenarium*, *Phytophthora capsici*, *Gaeumannomyces graminis var. tritici*, and *Sclerotinia sclerotiorum*, *Fusarium graminearum*) at 100 μg mL^{-1} are listed in Table 1 and Fig. 2. The results showed that most of the compounds exhibited certain to great inhibition activity against each of the fungi at 100 μg mL^{-1} (inhibition rate = 46.0–95.8%). Particularly, the antifungal activity of compounds **2-3–4**, **2-7–10**, **2-17**, **2-17–19**, **2-21**, **2-25–26**, **4-8–10**, **4-17**, **4-21**, and **4-25–26** was more potent than that of Tulipalin A and equal or higher than that of the natural product carabrone. Furthermore, from the results we can see that all the derivatives showed higher activity against *B. cinerea* and *G. graminis* (inhibition rate > 55%) compared to the other three pathogenic fungi.

According to these preliminary results, the half maximal inhibitory concentration (IC_{50}) of all the derivatives against *G. graminis* and *B. cinerea* was tested by the mycelial growth inhibitory rate method. It is notable that most of the γ-

Table 1 Initial antifungal activity of compounds at 100 μg mL[a]

Compound			Average inhibition rate (%) (100 μg mL^{-1}; 72 h)				
No.		R	*B. c.*	*C. l.*	*G. g.*	*S. s.*	*F. g.*
1	**2-1**	Ph	81.4 ± 0.7	76.7 ± 0.3	81.2 ± 0.8	63.2 ± 0.4	72.5 ± 0.2
2	**2-2**	2-PhCl	81.4 ± 0.5	77.9 ± 0.1	83.6 ± 0.4	68.7 ± 0.3	75.6 ± 0.4
3	**2-3**	3-PhCl	82.7 ± 0.8	77.6 ± 0.5	84.1 ± 0.2	69.1 ± 0.2	76.3 ± 0.5
4	**2-4**	4-PhCl	85.6 ± 0.8	80.1 ± 0.6	86.8 ± 0.2	72.3 ± 0.4	76.0 ± 0.1
5	**2-5**	2-PhBr	78.5 ± 0.2	72.3 ± 0.3	81.6 ± 0.7	63.6 ± 0.5	68.5 ± 0.3
6	**2-6**	3-PhBr	79.1 ± 0.7	74.9 ± 0.8	80.2 ± 0.4	65.4 ± 0.7	70.9 ± 0.5
7	**2-7**	4-PhBr	82.6 ± 0.5	78.6 ± 0.3	83.2 ± 0.5	66.3 ± 0.2	71.2 ± 0.5
8	**2-8**	2-PhF	86.3 ± 0.1	80.5 ± 0.5	91.7 ± 0.3	72.4 ± 0.5	77.3 ± 0.4
9	**2-9**	3-PhF	92.6 ± 0.3	87.5 ± 0.5	93.3 ± 0.5	75.5 ± 0.7	80.8 ± 0.6
10	**2-10**	4-PhF	95.8 ± 0.4	90.4 ± 0.5	95.1 ± 0.2	76.2 ± 0.1	82.2 ± 0.1
11	**2-11**	2-PhCH$_3$	73.3 ± 0.6	68.3 ± 0.2	75.5 ± 0.3	58.6 ± 0.3	63.6 ± 0.8
12	**2-12**	3-PhCH$_3$	75.6 ± 0.3	70.8 ± 0.5	73.6 ± 0.4	56.2 ± 0.2	61.4 ± 0.3
13	**2-13**	4-PhCH$_3$	77.6 ± 0.8	81.2 ± 0.1	77.6 ± 0.4	58.6 ± 0.3	64.5 ± 0.2
14	**2-14**	2-PhCH$_3$O	69.7 ± 0.8	64.5 ± 0.3	71.2 ± 0.1	53.4 ± 0.3	60.6 ± 0.5
15	**2-15**	3-PhCH$_3$O	72.6 ± 0.5	68.1 ± 0.4	76.6 ± 0.6	52.4 ± 0.7	56.6 ± 0.7
16	**2-16**	4-PhCH$_3$O	73.4 ± 0.2	69.8 ± 0.2	74.4 ± 0.3	55.3 ± 0.9	61.5 ± 0.4
17	**2-17**	4-PhCF$_3$	96.1 ± 0.7	91.3 ± 0.6	93.9 ± 0.5	79.8 ± 0.7	83.1 ± 0.5
18	**2-18**	2-C$_{10}$H$_7$	85.2 ± 0.3	80.5 ± 0.7	84.4 ± 0.3	71.3 ± 0.6	75.5 ± 0.2
19	**2-19**	9-C$_{14}$H$_9$	87.1 ± 0.8	81.3 ± 0.7	84.8 ± 0.6	72.2 ± 0.3	68.9 ± 0.4
20	**2-20**	4-PhCN	75.2 ± 0.8	71.3 ± 0.1	76.2 ± 0.7	65.1 ± 0.3	62.3 ± 0.8
21	**2-21**	2,4-PhCl$_2$	88.2 ± 0.7	82.6 ± 0.5	88.4 ± 0.3	74.5 ± 0.7	78.2 ± 0.7
22	**2-22**	2-Furfural	81.6 ± 0.4	75.3 ± 0.3	73.6 ± 0.6	69.3 ± 0.8	73.5 ± 0.3
23	**2-23**	4-PhCH$_2$CH$_3$	72.4 ± 0.6	65.2 ± 0.8	71.2 ± 0.3	57.2 ± 0.4	63.2 ± 0.4
24	**2-24**	4-PhCH(CH$_3$)$_2$	69.7 ± 0.7	63.4 ± 0.1	71.2 ± 0.3	55.6 ± 0.2	60.0 ± 0.1
25	**2-25**	Cinnamyl	92.2 ± 0.5	87.2 ± 0.6	92.3 ± 0.7	75.6 ± 0.3	82.9 ± 0.4
26	**2-26**	α-Br-cinnamyl	96.0 ± 0.9	88.3 ± 0.9	92.8 ± 0.6	78.2 ± 0.7	83.1 ± 0.7
27	**4-1**	Ph	79.2 ± 0.4	73.4 ± 0.8	77.7 ± 0.3	56.2 ± 0.1	62.2 ± 0.8
28	**4-2**	2-PhCl	78.4 ± 0.8	74.3 ± 0.2	75.5 ± 0.4	61.8 ± 0.4	66.6 ± 0.3
29	**4-3**	3-PhCl	79.5 ± 0.8	74.4 ± 0.8	74.2 ± 0.3	61.3 ± 0.1	67.3 ± 0.2
30	**4-4**	4-PhCl	80.6 ± 0.4	75.4 ± 0.7	82.1 ± 0.5	68.2 ± 0.5	74.8 ± 0.9
31	**4-5**	2-PhBr	76.7 ± 0.9	70.7 ± 0.8	76.8 ± 0.9	58.3 ± 0.2	64.2 ± 0.5
32	**4-6**	3-PhBr	77.2 ± 0.4	72.5 ± 0.3	77.4 ± 0.5	61.8 ± 0.7	66.3 ± 0.8
33	**4-7**	4-PhBr	80.6 ± 0.5	74.1 ± 0.3	75.3 ± 0.2	61.4 ± 0.5	68.2 ± 0.7
34	**4-8**	2-PhF	83.1 ± 0.3	78.2 ± 0.1	85.2 ± 0.6	68.3 ± 0.2	80.8 ± 0.3
35	**4-9**	3-PhF	86.4 ± 0.8	81.5 ± 0.3	87.1 ± 0.5	70.1 ± 0.4	76.3 ± 0.1
36	**4-10**	4-PhF	89.5 ± 0.6	83.4 ± 0.8	89.5 ± 0.4	72.6 ± 0.8	77.6 ± 0.2
37	**4-11**	2-PhCH$_3$	69.9 ± 0.3	63.1 ± 0.2	68.7 ± 0.3	53.5 ± 0.3	59.2 ± 0.4
38	**4-12**	3-PhCH$_3$	71.2 ± 0.3	66.5 ± 0.7	83.6 ± 0.2	51.1 ± 0.3	57.3 ± 0.7
39	**4-13**	4-PhCH$_3$	74.1 ± 0.6	68.3 ± 0.7	72.3 ± 0.4	52.7 ± 0.6	58.8 ± 0.4
40	**4-14**	2-PhCH$_3$O	65.7 ± 0.6	64.6 ± 0.4	55.2 ± 0.5	48.8 ± 0.3	54.1 ± 0.6
41	**4-15**	3-PhCH$_3$O	68.2 ± 0.3	66.8 ± 0.2	66.5 ± 0.9	46.0 ± 0.9	48.4 ± 0.3
42	**4-16**	4-PhCH$_3$O	69.2 ± 0.5	63.7 ± 0.4	62.0 ± 0.6	50.4 ± 0.3	51.6 ± 0.7
43	**4-17**	4-PhCF$_3$	91.4 ± 0.7	87.9 ± 0.6	87.3 ± 0.1	74.2 ± 0.1	75.2 ± 0.6
44	**4-18**	2-C$_{10}$H$_7$	80.2 ± 0.8	74.1 ± 0.8	78.4 ± 0.2	66.6 ± 0.7	71.1 ± 0.2
45	**4-19**	9-C$_{14}$H$_9$	81.6 ± 0.9	78.5 ± 0.3	77.5 ± 0.1	65.4 ± 0.3	70.3 ± 0.8
46	**4-20**	4-PhCN	69.5 ± 0.5	61.8 ± 0.5	78.7 ± 0.2	61.2 ± 0.1	63.6 ± 0.6
47	**4-21**	2,4-PhCl$_2$	83.4 ± 0.5	78.9 ± 0.6	83.6 ± 0.9	69.6 ± 0.5	75.4 ± 0.9
48	**4-22**	2-Furfural	76.5 ± 0.8	72.5 ± 0.3	65.6 ± 0.2	63.4 ± 0.8	69.2 ± 0.6
49	**4-23**	4-PhCH$_2$CH$_3$	70.8 ± 0.2	65.4 ± 0.4	63.2 ± 0.4	52.5 ± 0.4	56.5 ± 0.8
50	**4-24**	4-PhCH(CH$_3$)$_2$	68.2 ± 0.6	62.2 ± 0.6	55.3 ± 0.5	50.6 ± 0.9	53.6 ± 0.3
51	**4-25**	Cinnamyl	85.0 ± 0.3	80.4 ± 0.2	87.6 ± 0.5	71.1 ± 0.4	77.3 ± 0.5
52	**4-26**	α-Br-cinnamyl	86.6 ± 0.2	83.1 ± 0.2	86.2 ± 0.4	72.6 ± 0.3	80.1 ± 0.7
53	Carabrone		82.2 ± 0.7	75.6 ± 0.7	86.9 ± 0.7	71.3 ± 0.7	68.2 ± 0.7
54	Tulipalin A		64.9 ± 0.7	57.3 ± 0.7	68.3 ± 0.7	59.2 ± 0.7	56.5 ± 0.7

[a] *B. c.*, *Botrytis cinerea*; *C. l.*, *Colletotrichum lagenarium*; *G. g.*, *Gaeumannomyces graminis var. tritici*; *S. s.*, *Sclerotinia sclerotiorum*; *F. g.*, *Fusarium graminearum*.

butyrolactone derivates (IC_{50} = 14.54–134.56 μM) showed a superior activity against *G. graminis* compared to the δ-valerolactone derivates (IC_{50} = 24.45–154.88 μM), which might be plausibly ascribed to the intrinsic biological feature of the lactone ring and the fact that the γ-butyrolactone derivates bear conformation core size for receptor binding sites; on the

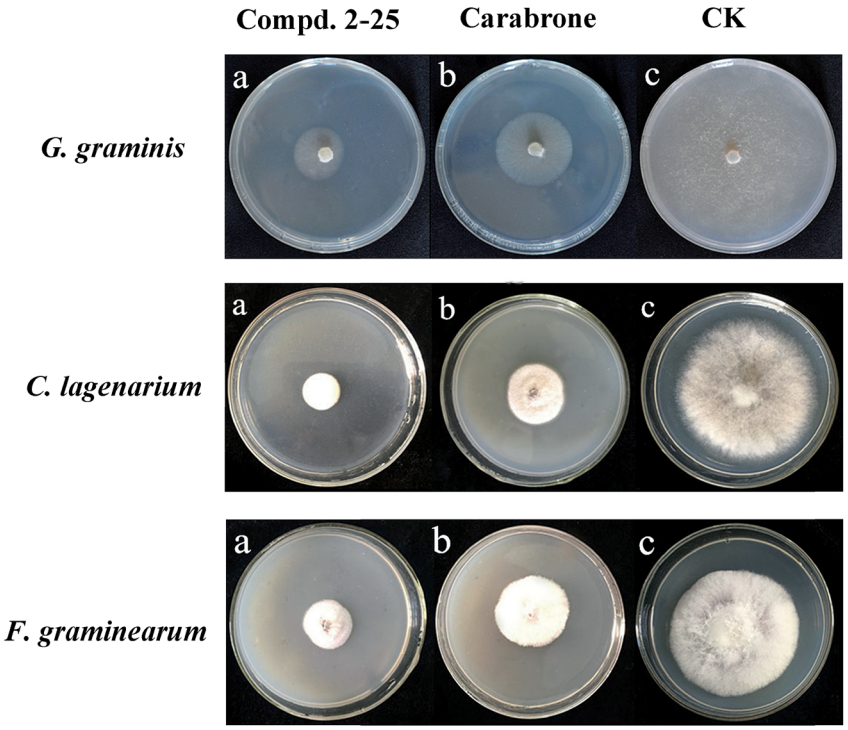

Fig. 2 *In vitro* antifungal activity of compounds against *Gaeumannomyces graminis var. tritici*, *Colletotrichum lagenarium* and *Fusarium graminearum* at 100 μg mL^{-1}.

contrary, the δ-valerolactone derivates disrupt the bioactive conformation. In order to investigate the SARs of the substituents on the lactone ring, different kinds and positions of substituent were introduced, and *G. graminis* was selected for SAR research for all compounds. According to the data in Table 2, we can construct SARs from the preliminary conclusions. The compounds **2-2–10** and **4-2–10** containing a halogen atom (-PhF, -PhCl, and -PhBr) exhibited obviously potent antifungal activity compared to the -$PhCH_3O$ and -$PhCH_3$ derivatives, which maybe due to the former derivates containing the electron-withdrawing group being beneficial to antifungal activity. In general, the activity of the compounds follows: F > Cl > Br > CH_3 > CH_3O. Remarkably, **2-17** displayed an IC_{50} value of 14.78 μM, an involved the -$PhCF_3$ electron-withdrawing substituent, the value was higher than that of the isopropyl (**2-24**, IC_{50} = 123.75 μM) and ethyl substituent (**2-23**, IC_{50} = 104.21 μM). In contrast with **2-17**, disubstitution of the benzylidene ring with a 2,4-$PhCl_2$ substituent did not improve activity, as seen from compound **2-21** (IC_{50} = 33.85 μM). A plausible explanation on such a decrease assumes that the steric effect interferes with receptor binding when a Cl atom is on the *ortho*-position.

As we can see, the steric effect also played an essential role for the antifungal activity. For the title compounds, substitution at the *para*-position was strongly favored over the corresponding *meta*- and/or *ortho*-positions, which was verified between the derivatives **2-2–16** and **4-2–16**, and the derivatives **2-2** (2-PhCl, IC_{50} = 45.45 μM) and **2-5** (2-PhBr, IC_{50} = 46.65 μM) were less potent than the corresponding derivatives **2-4** (4-PhCl, IC_{50} = 21.54 μM) and **2-7** (4-PhBr, IC_{50} = 33.64 μM). Meanwhile, with the bulky aryl groups, the derivatives (**2-18–19** and **4-18–19**) bearing a 2′-naphthyl or a 9′-anthryl group have no obvious increase in activity (IC_{50} = 47.85, 50.54, 75.25, 70.74 μM). Moreover, isopropyl with a bulky substituent was unfavorable to the activity. Taken together, these results could demonstrate the importance of substituents with a proper size, the *para*-position and the electron-withdrawing characteristic. Compared with aromatic substituent compounds **2-1** and **4-1** (IC_{50} = 88.21, 102.41 μM), a small decrease in activity was observed for compounds **2-22** and **4-22** (IC_{50} = 98.74, 114.36 μM) with the 2-furfural substituent. Unexpectedly, the cinnamic aldehyde compounds **2-25–26** and **4-25–26** (IC_{50} = 14.54, 16.44, 24.45, and 27.02 μM) showed higher antifungal activity toward *G. graminis* than other compounds and the natural product carabrone (IC_{50} = 28.54 μM), and derivatives **2-25** also displayed approximately 2-fold more activity than carbendazim (IC_{50} = 7.84 μM). This phenomenon may be due to the cinnamic aldehyde structure have some antifungal capability.

In vivo fungicidal bioactivity

In order to further confirm the antifungal activity of these title compounds, the *in vivo* fungicidal activities (protective effect) of the 14 promising derivatives were tested against *B. cinerea* on tomato fruits and against *G. graminis* and *B. graminis* on wheat seedlings.

As can be seen in Table 3 and Fig. 3, the inhibitory rates of compounds **2-10** and **2-25** exceed 80% against all three fungi at 200 μg mL^{-1}, meanwhile, compound **2-25** is equivalent with

Table 2 *In vitro* fungicidal activity of compounds against *B. cinerea* and *G. graminis*[a]

R	Compd	*G. graminis* IC_{50}, μM	*B. cinerea* IC_{50}, μM	*B. cinerea* pIC_{50}[c]	Compd	*G. graminis* IC_{50}, μM	*B. cinerea* IC_{50}, μM	*B. cinerea* pIC_{50}[c]
Ph	**2-1**	88.21	94.96	−1.98	**4-1**	102.41	119.26	−2.08
2-PhCl	**2-2**	45.45	63.50	−1.80	**4-2**	64.98	82.11	−1.91
3-PhCl	**2-3**	34.87	50.14	−1.70	**4-3**	51.20	79.00	−1.90
4-PhCl	**2-4**	21.54	46.39	−1.67	**4-4**	48.58	66.44	−1.82
2-PhBr	**2-5**	46.65	66.80	−1.83	**4-5**	66.73	83.58	−1.92
3-PhBr	**2-6**	41.76	58.54	−1.77	**4-6**	64.54	78.47	−1.89
4-PhBr	**2-7**	33.64	50.92	−1.71	**4-7**	51.41	70.12	−1.85
2-PhF	**2-8**	45.47	49.31	−1.69	**4-8**	62.35	79.83	−1.90
3-PhF	**2-9**	28.52	39.26	−1.59	**4-9**	48.55	74.35	−1.87
4-PhF	**2-10**	20.15	28.33	−1.45	**4-10**	40.05	66.78	−1.82
2-$PhCH_3$	**2-11**	122.13	136.06	−2.13	**4-11**	124.38	165.43	−2.22
3-$PhCH_3$	**2-12**	98.47	127.45	−2.11	**4-12**	103.47	147.27	−2.17
4-$PhCH_3$	**2-13**	78.77	107.72	−2.03	**4-13**	96.24	130.25	−2.11
2-$PhCH_3O$	**2-14**	134.54	145.29	−2.16	**4-14**	154.88	175.22	−2.24
3-$PhCH_3O$	**2-15**	115.64	138.43	−2.14	**4-15**	126.37	173.16	−2.24
4-$PhCH_3O$	**2-16**	104.12	131.62	−2.12	**4-16**	123.24	153.30	−2.19
4-$PhCF_3$	**2-17**	14.78	21.65	−1.34	**4-17**	31.38	56.00	−1.75
2-$C_{10}H_7$	**2-18**	47.85	57.88	−1.76	**4-18**	75.25	89.55	−1.95
9-$C_{14}H_9$	**2-19**	50.54	39.84	−1.60	**4-19**	70.74	60.88	−1.78
4-PhCN	**2-20**	87.76	106.80	−2.03	**4-20**	98.54	135.50	−2.13
2,4-$PhCl_2$	**2-21**	33.85	42.77	−1.63	**4-21**	55.98	65.04	−1.81
2-Furfural	**2-22**	98.74	113.69	−2.06	**4-22**	114.36	133.45	−2.13
4-$PhCH_2CH_3$	**2-23**	104.21	145.63	−2.16	**4-23**	148.47	163.54	−2.21
4-$PhCH(CH_3)_2$	**2-24**	123.75	152.10	−2.18	**4-24**	142.55	176.65	−2.25
Cinnamyl	**2-25**	14.54	23.73	−1.38	**4-25**	24.45	38.95	−1.84
α-Br-cinnamyl	**2-26**	16.44	21.12	−1.32	**4-26**	27.02	46.17	−1.66
Tulipalin A		58.27	67.86	—	Carabrone	28.54	25.74	—
Carbendazim[b]		7.84	8.34	—	—	—	—	—

[a] All half maximal inhibitory concentration (IC_{50}) values are presented as the mean ± SD ($n = 3$), μM. [b] Commercial fungicide, carbendazim was used as the positive control. [c] pIC_{50}, the tested IC_{50} values were converted into the corresponding plog IC_{50} values.

Table 3 *In vivo* fungicidal activity (protective effect) of compounds against *B. cinerea*, *G. graminis* and *B. graminis*[a]

No.	Compounds (200 μg mL^{-1})	Against *B. cinerea* (%)	Against *G. graminis* (%)	Against *B. graminis* (%)
1	**2-2**	52.21d	57.65d	56.36d
2	**2-10**	82.43ab	83.59a	81.67a
3	**2-13**	61.23cd	59.65d	52.34d
4	**2-17**	78.65b	81.54ab	78.65ab
5	**2-19**	56.54d	41.68e	42.52e
6	**2-21**	55.65d	66.58c	64.38c
7	**2-23**	66.51c	48.68e	51.25d
8	**2-25**	86.61a	85.67a	80.24a
9	**4-1**	56.42d	52.24d	46.75e
10	**4-7**	77.85b	70.36b	73.51b
11	**4-15**	56.24d	62.87c	46.27
12	**4-18**	68.57c	66.34c	59.68d
13	**4-20**	66.33c	62.24c	57.46d
14	**4-25**	80.47ab	76.39b	79.38ab
15	Tulipalin A	54.21d	58.36d	42.94e
16	Carabrone	70.36bc	80.24ab	73.58b
17	Triadimefon	—	87.29a	82.39a
18	Carbendazim	89.54a	—	—

[a] Values are the means of three replicates; letters a–d represent a significant difference at $p = 0.05$; commercial fungicide, triadimefon and carbendazim were used as the positive control.

commercial fungicide (carbendazim or triadimefon). Compounds **2-17** and **4-7** also showed great activity, and their protective inhibitory rates were higher than 70%. The above results indicated that the *in vivo* fungicidal activities in this research were aligned with *in vitro* activities; moreover, the *in vivo* fungicidal activities were better than the *in vitro* activity.

QSAR study and antifungal activity against *B. cinerea*

Conformer optimization and minimum energy calculations are the essential procedures in the construction of a QSAR model. In this paper, 52 γ-butyrolactone and δ-valerolactone compounds were used as samples and 5 groups of descriptors were obtained. Heuristic regression was chosen to acquire a QSAR model with satisfactory values of R^2, F, and S^2, which were used to establish a relationship between antifungal activity and molecular descriptors.

The number of descriptors was achieved by the "breaking point" rule, and according to the t values in the test, the descriptors were obtained. Meanwhile, the numbers of samples and descriptors also meet the equation $3D \leq S - 3$ (S means the number of samples; D means the number of descriptors). At last, the final 5-descriptor model was generated. In the ESI,† the

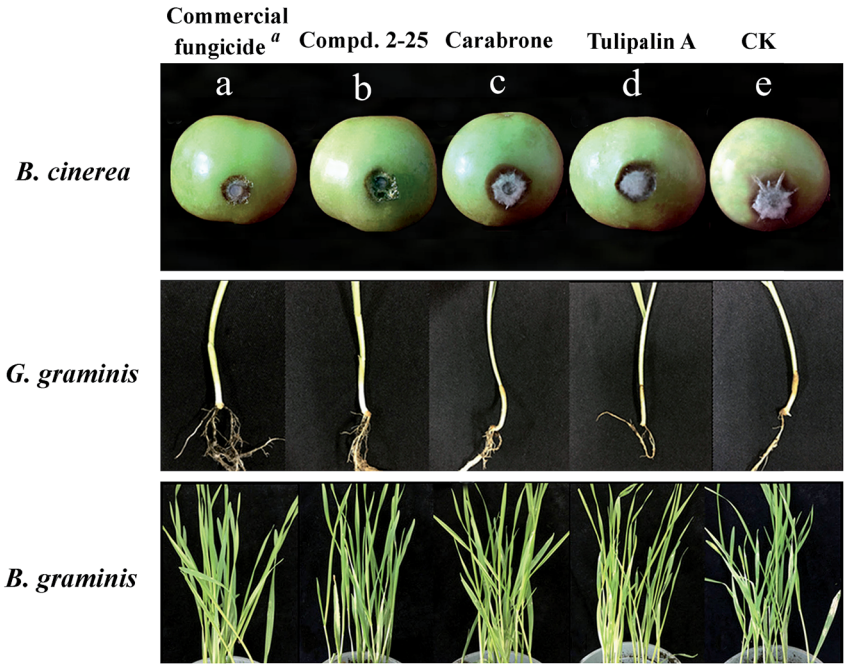

Fig. 3 *In vivo* antifungal activity of compounds against *Botrytis cinerea*, *Gaeumannomyces graminis var. tritici*, and *Blumeria graminis* at 200 μg mL^{-1}. [a]Commercial fungicide; carbendazim was used as the *B. cinerea* positive control and triadimefon was used as the *G. graminis* and *B. graminis* positive control.

five significant descriptors, the "breaking point" rule figure and their values are listed.

The fabricated QSAR model equation has five descriptors presented in a grading down way based on the importance of the statistical analysis, as shown in Table 4. According to this optimized model, the comparison chart of the predictive and practical activity of the 52 compounds was exhibited in Fig. 4. Compared with experimental pIC_{50} (negative log IC_{50}), we could conclude that the generated model was reliable. The final QSAR model with 5 descriptors can be described as

$$pIC_{50} = -4.6536 + 5.4325 \times q^{O}_{max.} - 3.1128 \times n_o + 2.5461 \times MAOEP + 0.0665 \times \mu_c - 3.5452 \times q_{max.},$$
$$N = 52,\ R^2 = 0.947,\ F = 65.77,\ S^2 = 0.0028$$

Internal validation and "leave-one-out" cross-validation methods were carried out to validate the established QSAR model.[32] Internal validation results were presented in the ESI.† The $R_{Training}^2$ and R_{Test}^2 were within 5% for all three sets, and the average values of $R_{Training}^2$ and R_{Test}^2 approached the overall R^2 value. So, the obtained QSAR model indicated the predictive power of 3-fold cross-validation. In the "leave-one-out" method, every fourth compound **1**, **5**, **9**, *etc.*, was an external test set, and the others were the training set. The R^2 values of the training set and test set were close, and the QSAR model acquired in this study was available.

By explaining the descriptors of this model, we could gain some insight into the structural features and antifungal activity. The 1st and 5th descriptors obtained in this study were the max. net atomic charge for an O atom and the max. net atomic

Table 4 The best five-descriptor model

Descriptor no.	X	$\pm\Delta X$	t-Text	Descriptor
0	−4.6536	3.2135×10^{-1}	6.6525	Intercept
1	5.4325	3.4576×10^{-1}	−2.7665	$q^{O}_{max.}$ [a]
2	3.1128	5.7687	−1.6532	n_o [b]
3	2.5461	1.0893	2.6675	MAOEP [c]
4	6.6523×10^{-2}	3.2254×10^{-2}	1.9878	μ_c [d]
5	3.5452	2.2153×10^{-1}	2.6673	$q_{max.}$ [e]

[a] Max. net atomic charge for an O atom. [b] Number of occupied electronic levels of atoms. [c] Max. atomic orbital electronic population. [d] Total point-charge composition of the molecular dipole. [e] Max. net atomic charge.

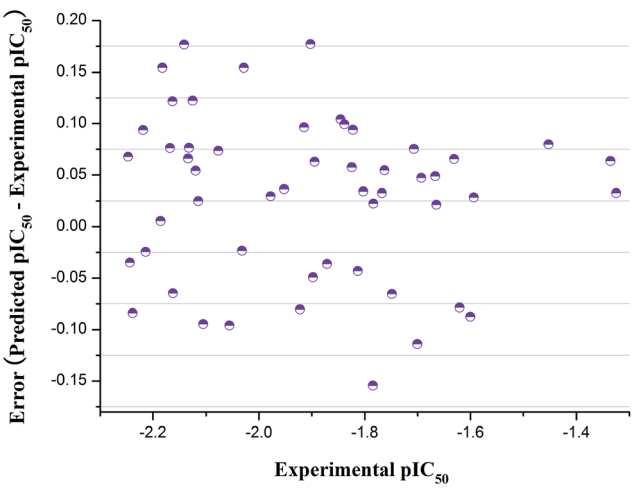

Fig. 4 Graphic of pEC_{50} values *versus* respective errors.

charge. These two descriptors belonged to electrostatic descriptors and they reflect the charge distribution of the molecules as shown in the contour maps indicating the occupied electronic levels of compounds **2-4** and **4-17** (Fig. 5), which represent the geometric mean of atomic electronegativities.[33,34] According to the frontier molecular orbital theory (FMO) of chemical reactivity, the formation of a transition state is due to an interaction between the frontier orbitals (HOMO and LUMO) of the reacting species. So the electrostatic properties of an O atom and max. net atomic charge were important elements for the antifungal activity of the title compounds.

The second and third most important descriptors obtained in this model were the maximum atomic orbital electronic population and the number of occupied electronic levels of atoms. The former is an important descriptor to reflect the nucleophilicity of the molecule, which is directly in contact with the molecular nucleophilic capacity and describes the susceptibility of the molecule to electrophilic attack.[35] The number of occupied electronic levels of atoms belongs to quantum-chemical descriptors, which therefore act directly on the quantum chemically calculated charge distribution in the molecules and describes the molecular polar interactions. Meanwhile, as the result of the of electron activity difference between the atoms, the optimized geometries and permanent polarization are shown in the molecular electrostatic potential map simultaneously (Fig. 5), and we can see that the exocyclic carbon–carbon double bond exhibits greater negative electrostatic potential which easily occurred in the nucleophilic reaction.[36,37] Actually, α-methylene-γ-butyrolactone derivatives with

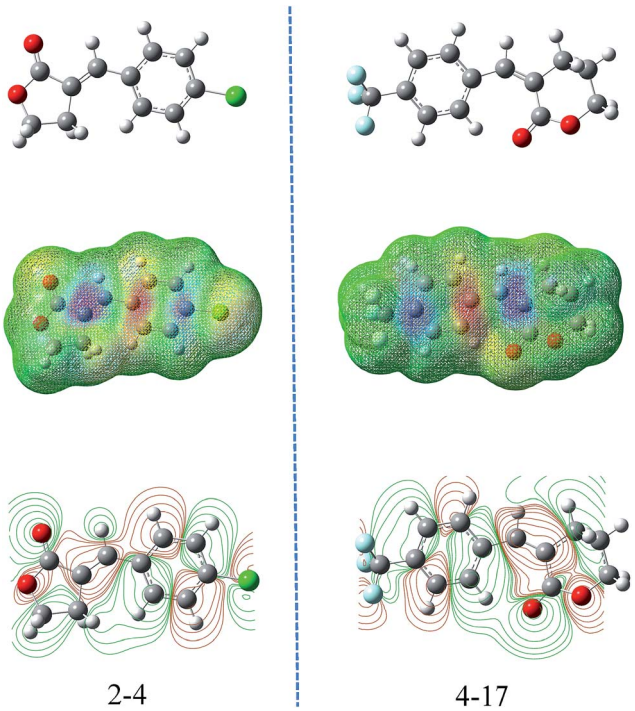

Fig. 5 Molecular electrostatic potential and contour maps of compounds **2-4** and **4-17**. The green parts represent positive molecular orbitals, and the red parts represent negative molecular orbitals.

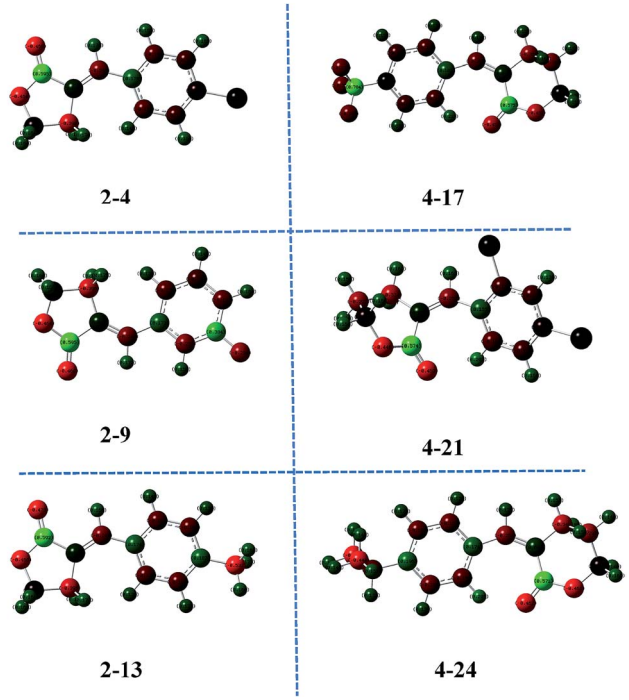

Fig. 6 Optimized geometries and charge distribution of compounds **2-4**, **2-9**, **2-13**, **4-17**, **4-21**, and **4-24**.

an electrophilic α,β-unsaturated carbonyl system (Michael acceptor), which had higher electron deficiency, could react with biological nucleophiles.[38,39]

The fifth important descriptor was the total point-charge component of the molecular dipole (μ_c), which measured the hydrophilic/lipophilic property of the compounds.[40–42] The appropriate μ_c value illustrated the penetration ability of the molecules to the cell as well as interaction with the action target to a large extent. As shown in Fig. 6, the optimized geometries and charge distribution on the atoms of compounds **2-4**, **2-9**, **2-13**, **4-17**, **4-21** and **4-24** were demonstrated simultaneously. It was illustrated that, after lactone ring modification with aromatics, the hydrophilic and lipophilic property of the compounds was regulated, therefore the μ_c value was an essential factor in adjusting the antifungal activity.

Conclusion

Inspired by the bioactivity of sesquiterpene lactones and the natural product Tulipalin A, a series of α-methylene-γ-lactone and α-methylene-δ-lactone compounds were prepared through structural modification. The antifungal activity of all compounds against *G. graminis* and *B. cinerea* were evaluated, and the γ-lactone derivatives exhibited higher antifungal activity than the δ-lactone derivatives. Particularly, compound **2-25** connected with a cinnamic aldehyde structure showed superior *in vitro* and *in vivo* fungicide activities. The SAR indicated that electron-withdrawing groups and steric effects played important roles simultaneously. Moreover, the QSAR model ($R^2 = 0.947$, $F = 65.77$, and $S^2 = 0.0028$) indicated that the net

atomic charges, nucleophilicity and hydrophilic/lipophilic property of the compounds are the most important in this research. In view of these results, we know more about the antifungal activity of α-methylene-γ-lactone substructures, especially that compound **2-25** contains a γ-butyrolactone scaffold and cinnamic aldehyde moiety and has the potential to be a fungicide candidate.

Conflicts of interest

The authors have no conflicts of interest to declare.

Acknowledgements

We greatly appreciate the funding support for this research provided by the National Natural Science Foundation of China (No. 31471800). We also thank the Kunming Institute of Botany, Chinese Academy of Science for the HR-MS spectral data.

References

1 M. Ishtiaq, M. A. Saleem and M. Razaq, *Crop Prot.*, 2012, **33**, 13–20.
2 P. K. Anderson, A. A. Cunningham, N. G. Patel, F. J. Morales, P. R. Epstein and P. Daszak, *Trends Ecol. Evol.*, 2004, **19**, 535–544.
3 F. E. Dayan, C. L. Cantrell and S. O. Duke, *Bioorg. Med. Chem.*, 2009, **17**, 4022–4034.
4 C. F. Nising, S. Hillebrand and L. Rodefeld, *Chem. Commun.*, 2011, **47**, 4062–4073.
5 L. G. Copping and B. P. Khambay, *Pest Manage. Sci.*, 2015, **56**, 649–650.
6 L. G. Copping, *Crop Prot.*, 1997, **16**, 491–492.
7 A. K. Picman, *Biochem. Syst. Ecol.*, 1986, **14**, 255–281.
8 M. F. Neerman, *Int. J. Aromather.*, 2003, **13**, 114–120.
9 G. Lyss, A. Knorre, T. J. Schmidt, H. L. Pahl and I. Merfort, *J. Biol. Chem.*, 1998, **273**, 33508–33516.
10 T. J. Schmidt, *Curr. Org. Chem.*, 1999, **3**, 577–608.
11 A. K. Picman, E. Rodriguez and C. H. N. Towers, *Chem.-Biol. Interact.*, 1979, **28**, 83–90.
12 P. M. Bork, M. L. Schmitz, M. Kuhnt, C. Escher and M. Heinrich, *FEBS Lett.*, 1997, **402**, 85–90.
13 J. Feng, H. Wang, S. Ren, J. He and X. Zhang, *J. Agric. Food Chem.*, 2012, **60**, 3817–3823.
14 J. Feng, D. Wang, Y. Wu, H. Yan and X. Zhang, *Bioorg. Med. Chem. Lett.*, 2013, **23**, 4393–4397.
15 Y. Wu, D. Wang, E. Guo, S. Song, J. Feng and X. Zhang, *Bioorg. Med. Chem. Lett.*, 2017, **27**, 1284–1290.
16 J. Lee, J. Lee, J. Lim, S. Sim and D. Park, *J. Med. Plants Res.*, 2008, **2**, 059–065.
17 T. Janecki, E. Błaszczyk, K. Studzian, A. Janecka, U. Krajewska and M. Rozalski, *J. Med. Chem.*, 2005, **48**, 3516–3521.
18 I. G. Shibi, L. Aswathy, R. S. Jisha, V. H. Masand, A. Divyachandran and J. M. Gajbhiye, *Eur. J. Med. Chem.*, 2015, **77**, 9–23.
19 C. Hansch and R. P. Verma, *Eur. J. Med. Chem.*, 2009, **44**, 260–273.
20 A. K. Mahalingam, A. Linda, K. E. Jenny, W. Johan, K. Jacob, T. Unge, W. Hans, M. Larhed and H. Anders, *J. Med. Chem.*, 2010, **53**, 607–615.
21 Y. Ru Meng and Y. D. Guan, *Chin. Chem. Lett.*, 2002, **13**, 1039–1042.
22 S. Brase, A. Encinas, J. Keck and C. F. Nising, *Chem. Rev.*, 2009, **109**, 3903–3990.
23 M. Wang, Q. Zhang, Q. Ren, X. Kong, L. Wang, H. Wang, J. Xu and Y. Guo, *J. Agric. Food Chem.*, 2014, **62**, 10945–10953.
24 L. Fang, M. Wang, S. Gou, X. Liu, H. Zhang and F. Cao, *J. Med. Chem.*, 2014, **57**, 1116–1120.
25 R. P. John, R. D. Tyagi, D. Prévost, S. K. Brar, S. Pouleur and R. Y. Surampalli, *Crop Prot.*, 2010, **29**, 1452–1459.
26 F. Chen, M. Wang, Y. Zheng, J. Luo, X. Yang and X. Wang, *World J. Microbiol. Biotechnol.*, 2010, **26**, 675–684.
27 M. J. Frisch, G. W. Trucks, H. B. Schlegel, G. E. Scuseria, M. A. Robb, J. R. Cheeseman, J. A. Montgomery, T. Vreven, K. N. Kudin and J. C. Burant, *Gaussian 03*, Gaussian, Inc., Wallingford, CT, USA, 2004.
28 A. Katritsky, M. Karelson, V. S. Lobanov, R. Dennington, T. A. Keith and R. D. A. T. Keith, *Codessa 2.7.15*, Semichem, Inc., Shawnee, KS, USA, 2004.
29 M. J. S. Dewar, A. J. Holder, I. Roy, D. Dennington, D. A. Liotard, D. G. Truhlar, T. A. Keith, J. M. Millam and C. D. Harris, *AMPAC 9.3.1*, Semichem, Inc., Shawnee, KS, USA, 2004.
30 Y. Gao, X. Tian, J. Li, S. Shang, Z. Song and M. Shen, *ACS Sustainable Chem. Eng.*, 2016, **4**, 2741–2747.
31 J. Li, X. Tian, Y. Gao, S. Shang, J. Feng and X. Zhang, *RSC Adv.*, 2015, **5**, 66947–66955.
32 A. Andreani, S. Burnelli, M. Granaiola, A. Leoni, A. Locatelli, R. Morigi, M. Rambaldi, L. Varoli, N. Calonghi and R. H. Shoemaker, *J. Med. Chem.*, 2008, **51**, 7508–7513.
33 A. Andreani, A. Locatelli, A. Leoni, M. Rambaldi, R. Morigi, R. Bossa, M. Chiericozzi, A. Fraccari and I. Galatulas, *Eur. J. Med. Chem.*, 1997, **32**, 919–924.
34 J. Li, Y. Gao, S. Shang, X. Rao, J. Song and Z. Wang, *RSC Adv.*, 2014, **4**, 58190–58199.
35 R. Kumar, A. Kumar, S. Jain and D. Kaushik, *Eur. J. Med. Chem.*, 2011, **46**, 3543–3550.
36 M. Witschel, *Bioorg. Med. Chem.*, 2009, **17**, 4221–4229.
37 L. Zhao and S. Feng, *J. Colloid Interface Sci.*, 2007, **274**, 55–68.
38 A. Cho, C. E. Song, S. K. Lee, W. S. Shin and E. Lim, *J. Mater. Sci.*, 2016, **51**, 6770–6780.
39 D. Sharma, B. Narasimhan, P. Kumar and A. Jalbout, *Eur. J. Med. Chem.*, 2009, **44**, 1119–1127.
40 P. Sharma, A. Kumar, S. Upadhyay, V. Sahu and J. Singh, *Eur. J. Med. Chem.*, 2009, **44**, 251–259.
41 K. Kalani, D. Yadav, F. Khan, S. Srivastava and N. Suri, *J. Mol. Model.*, 2012, **18**, 3389–3413.
42 T. J. Schmidt, A. M. M. Nour, S. A. Khalid, M. Kaiser and R. Brun, *Molecules*, 2009, **14**, 2062–2076.

